Auto-imunidade Celular

Prof. Dr. Jean Pierre Schatzmann Peron
Laboratório de Interações Neuroimunes

Precursores linfóides, agora chamados timócitos, migram da CÓRTEX PARA MEDULA e não expressam CD4 nem CD8

$CD4^{neg}$ $CD8^{pos}$

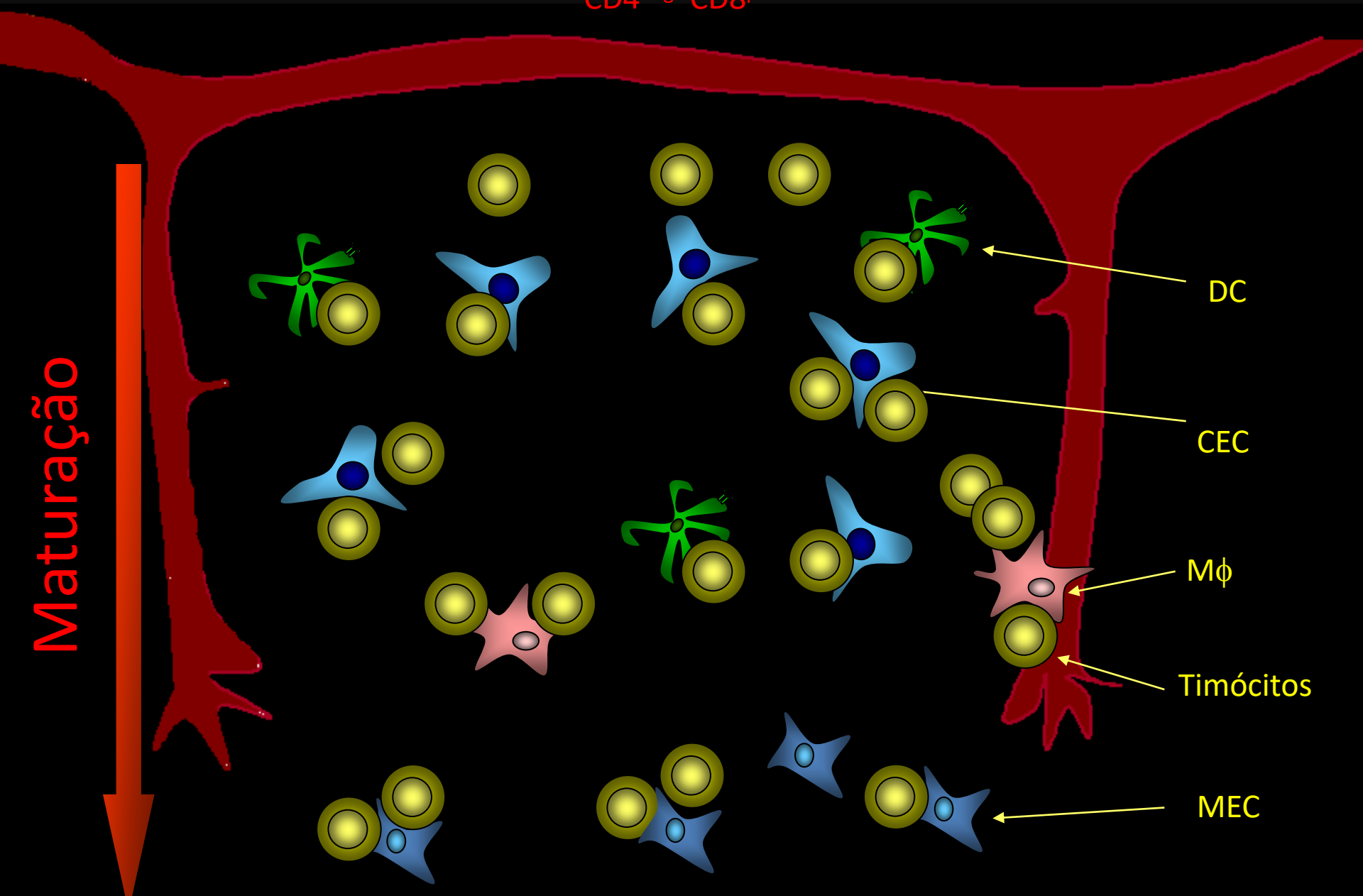

Ao adentrar o timo, timócitos passam a expressar $CD4^{pos}$ $CD8^{pos}$

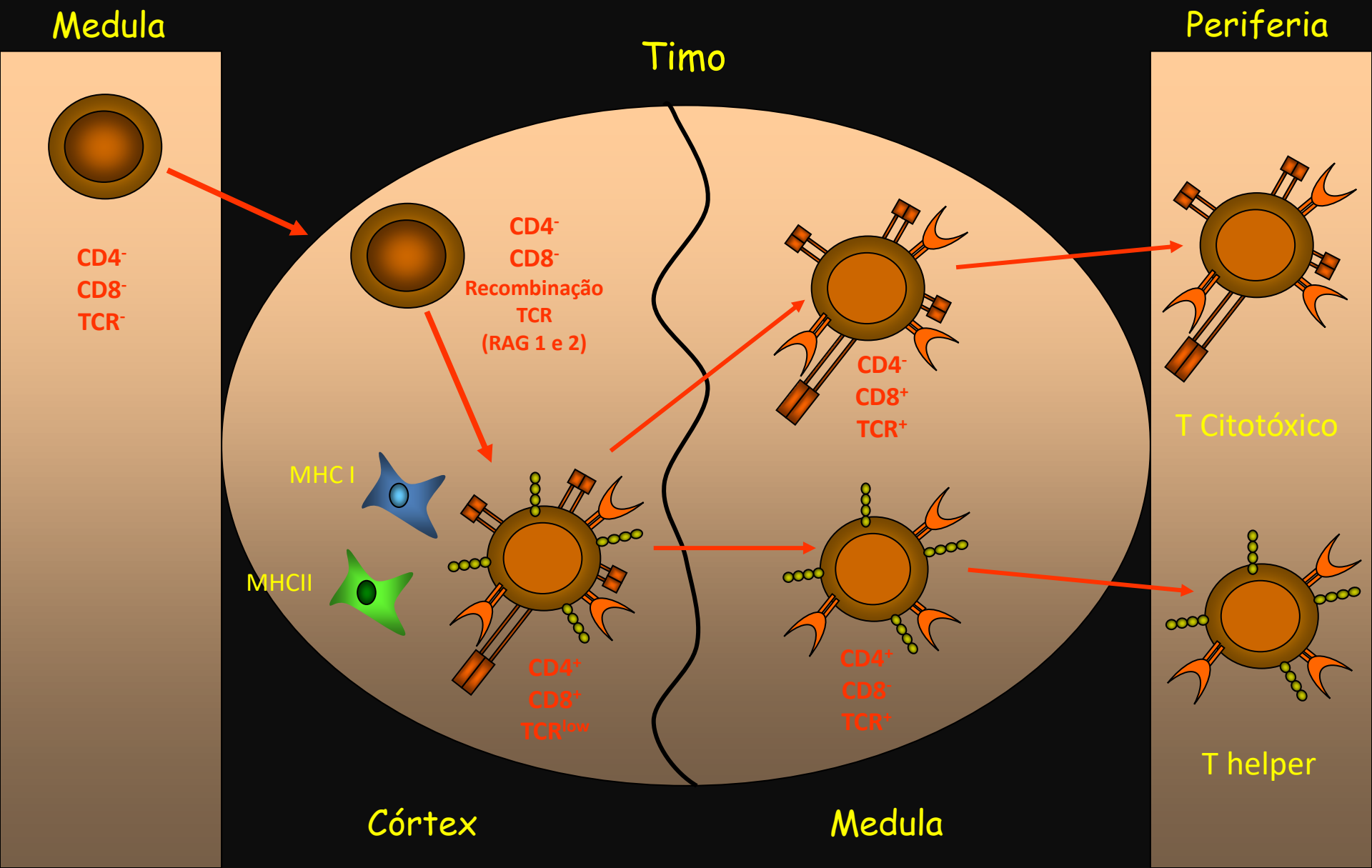

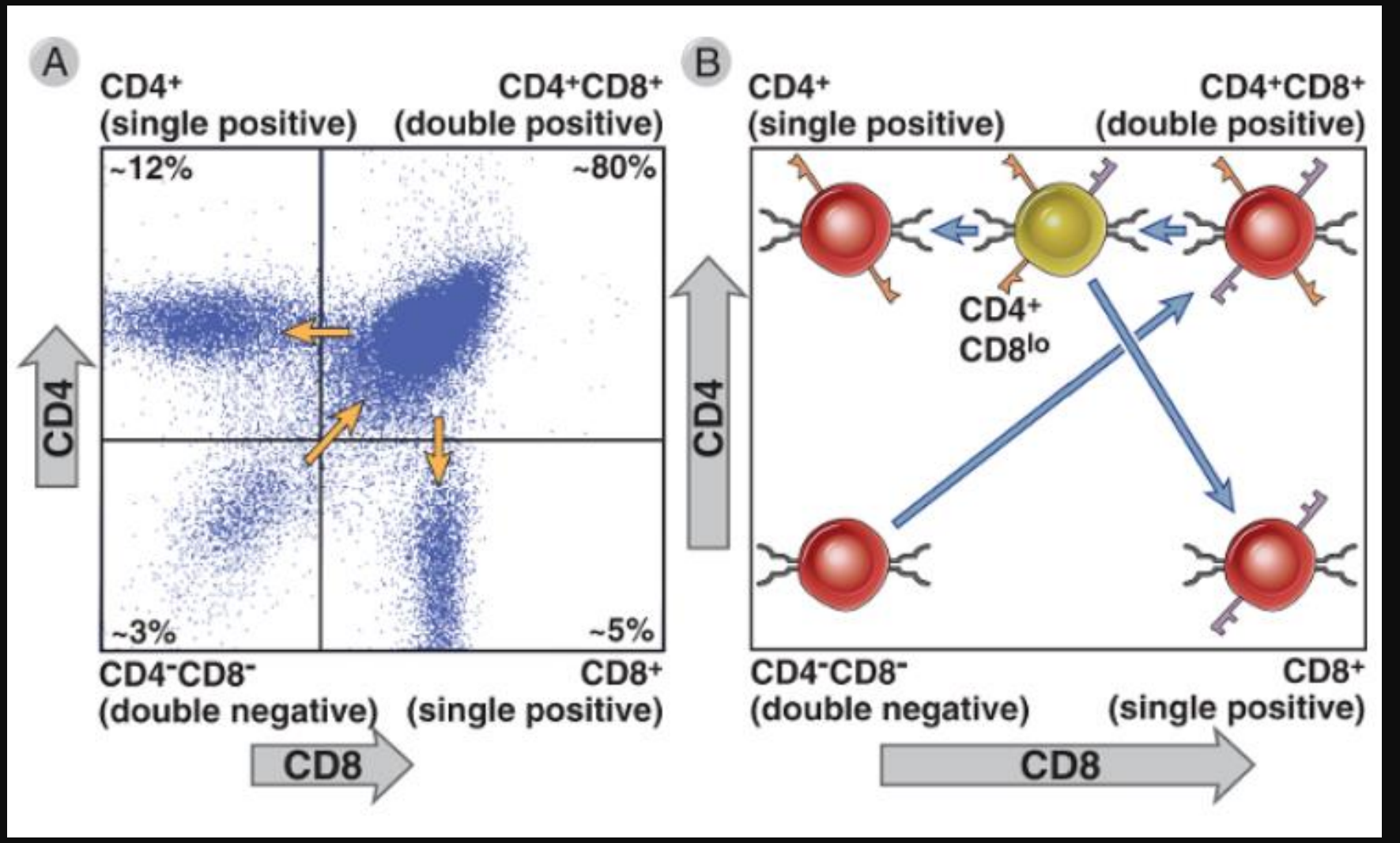
A
CD4+
(single positive)
CD4+CD8+
(double positive)
~12%
~80%
~3%
~5%
CD4-CD8-
(double negative)
CD8+
(single positive)
CD4
CD8
B
CD4+
(single positive)
CD4+CD8+
(double positive)
CD4+
CD8lo
CD4-CD8-
(double negative)
CD8+
(single positive)
CD4
CD8

Limiar de Seleção
Regido pela Força de Interação Entre os Linfócitos e Antígenos Próprios

Precursores linfóides, agora chamados timócitos, migram da CÓRTEX PARA MEDULA e não expressam CD4 nem CD8

$CD4^{neg}$ $CD8^{pos}$

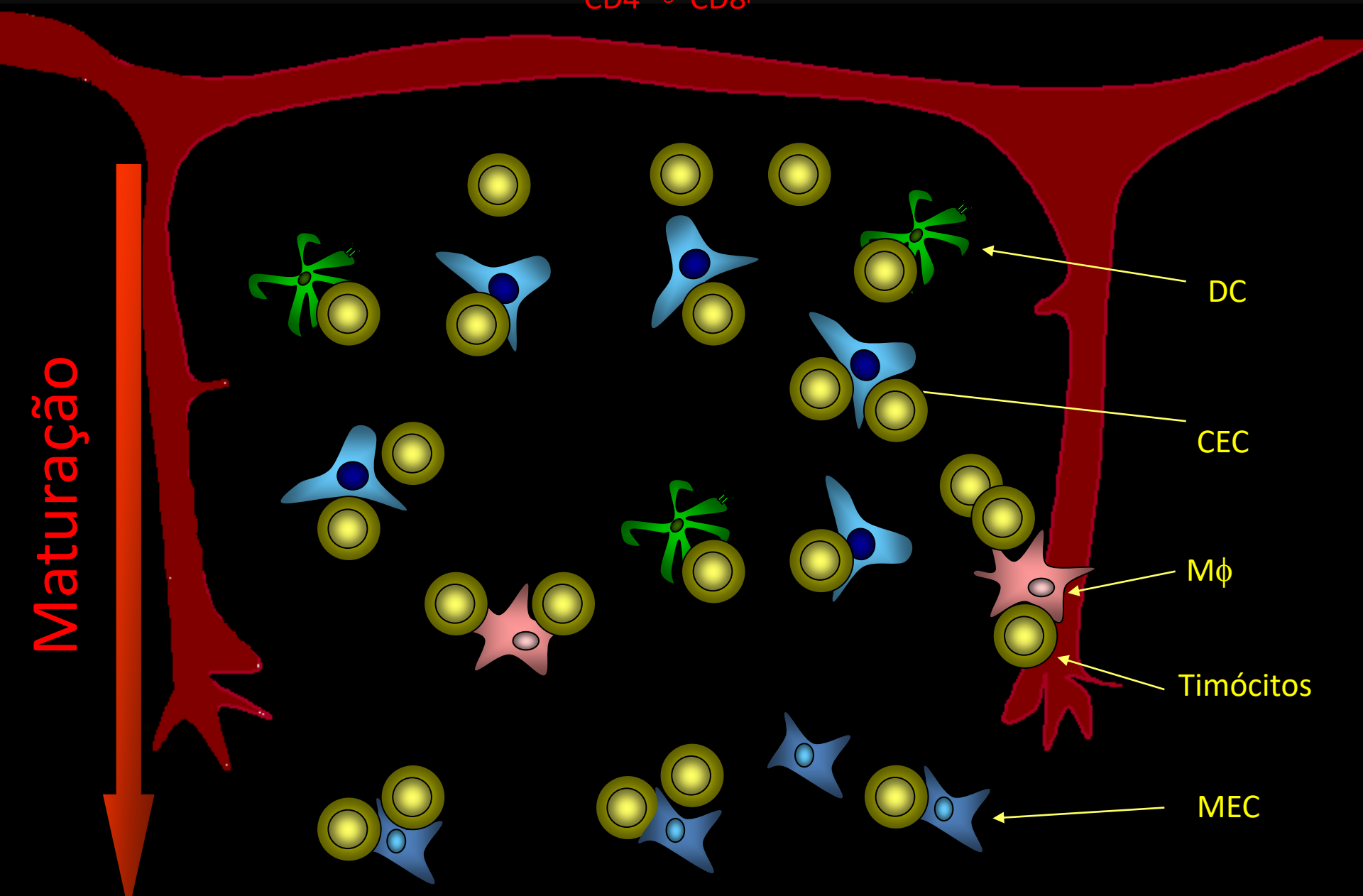

Loci do TCR

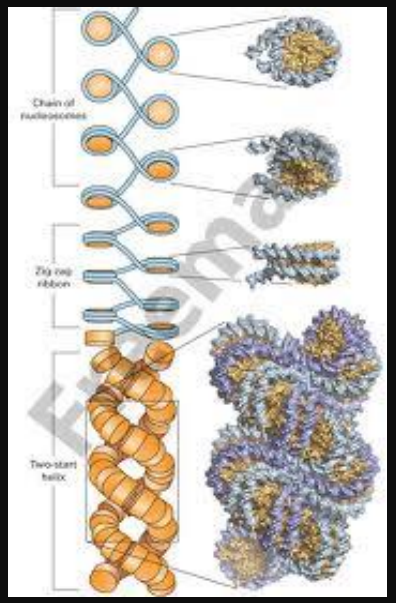

Imunologia Celular e Molecular
ISBN: 9788535222449
Elsevier Editora

Locus da cadeia β do TCR humano (620 kb; cromossomo 7)

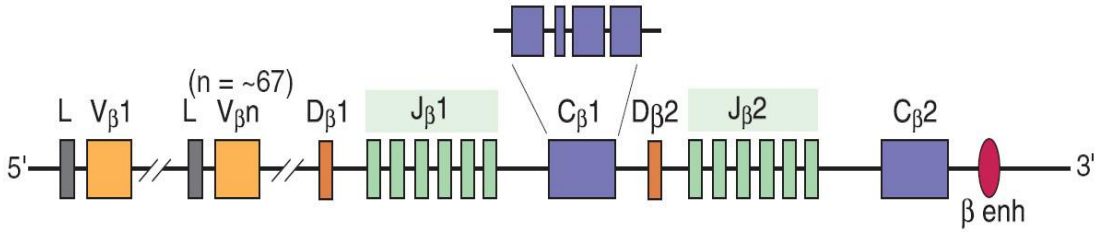

Locus das cadeias α e δ do TCR humano (1.000 kb; cromossomo 14)

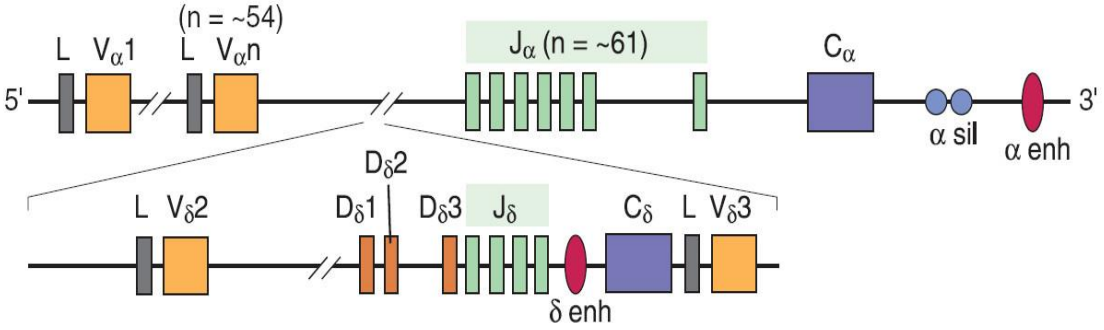

Locus da cadeia γ do TCR humano (200 kb; cromossomo 7)

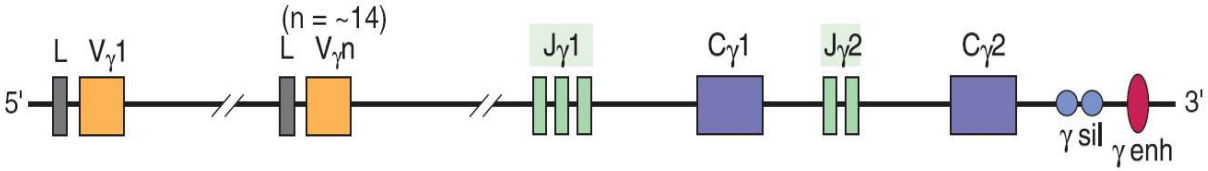

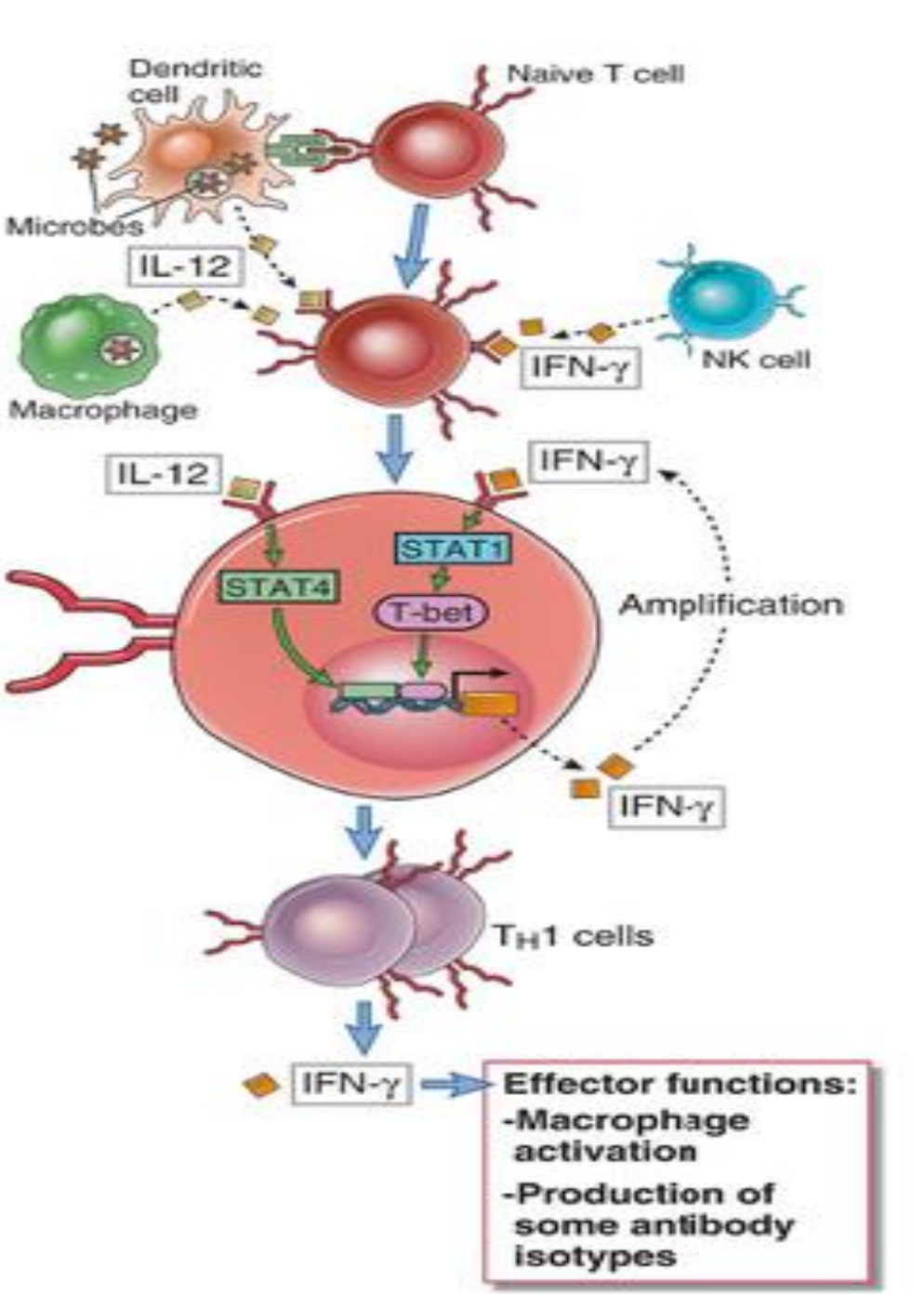

Resposta Th1

- Agentes Intra-celulares
- Ativação da Capacidade Fagocítica e de Degradação Intracelular
- Macrófagos Inflamatórios M1
- A tivação Células NK
- Citocinas principais
- IL-1, IL-12, IL-8, IL-18

IL-12, TNF-α, IFN-γ

Apresentação de Antígenos e Ativação dos Linfócitos T

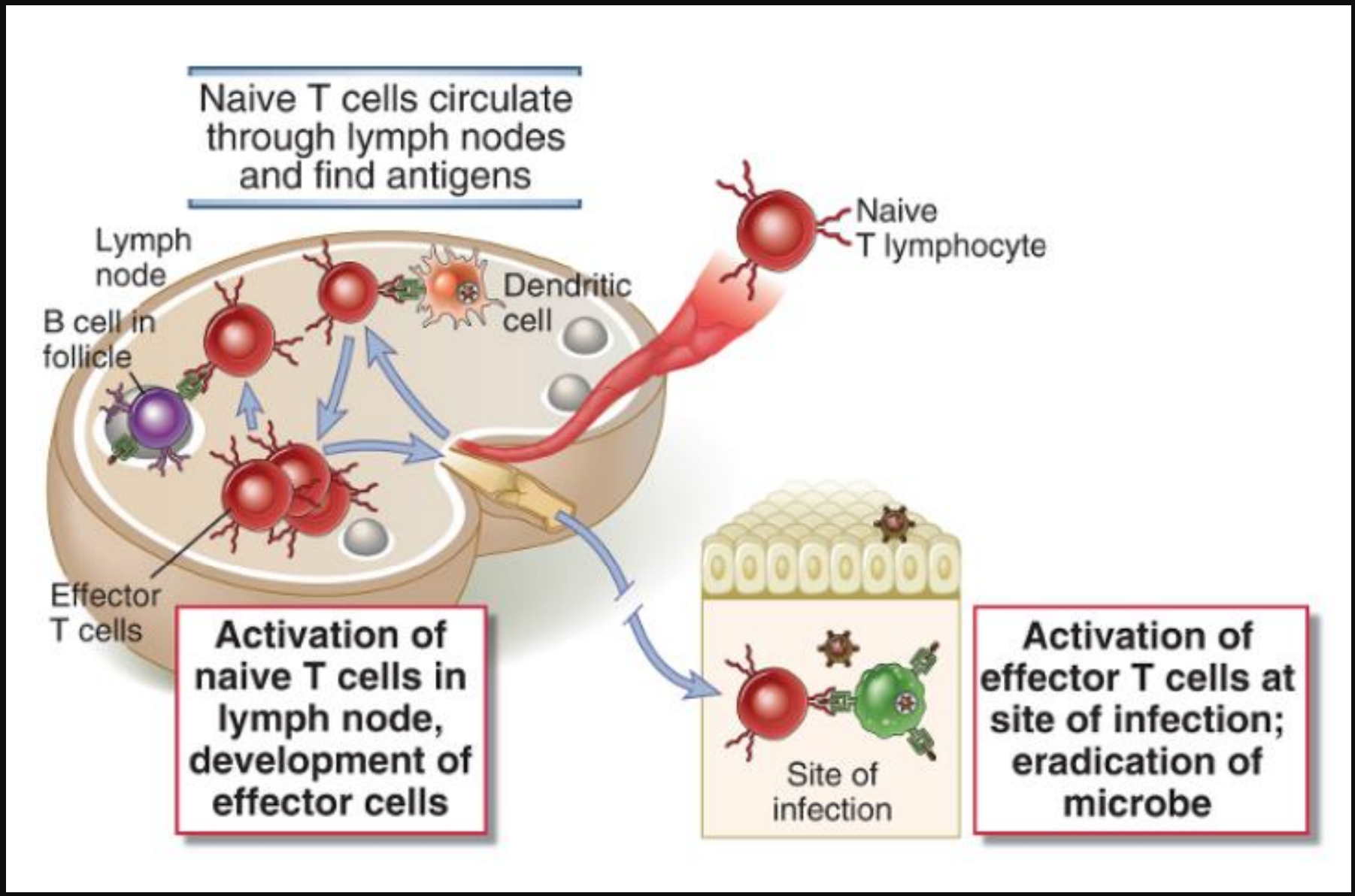

Quais eventos celulares são observados?

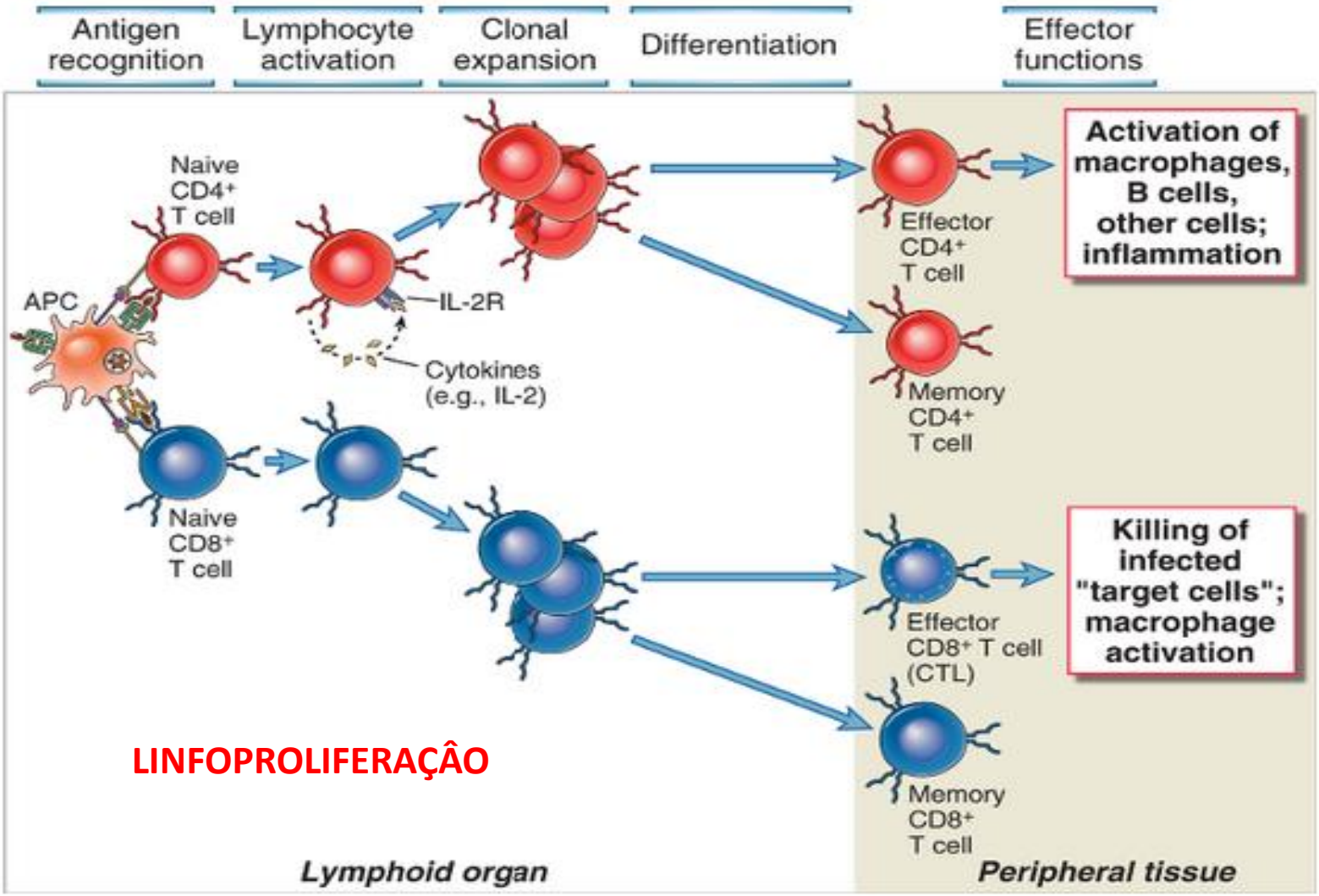

A

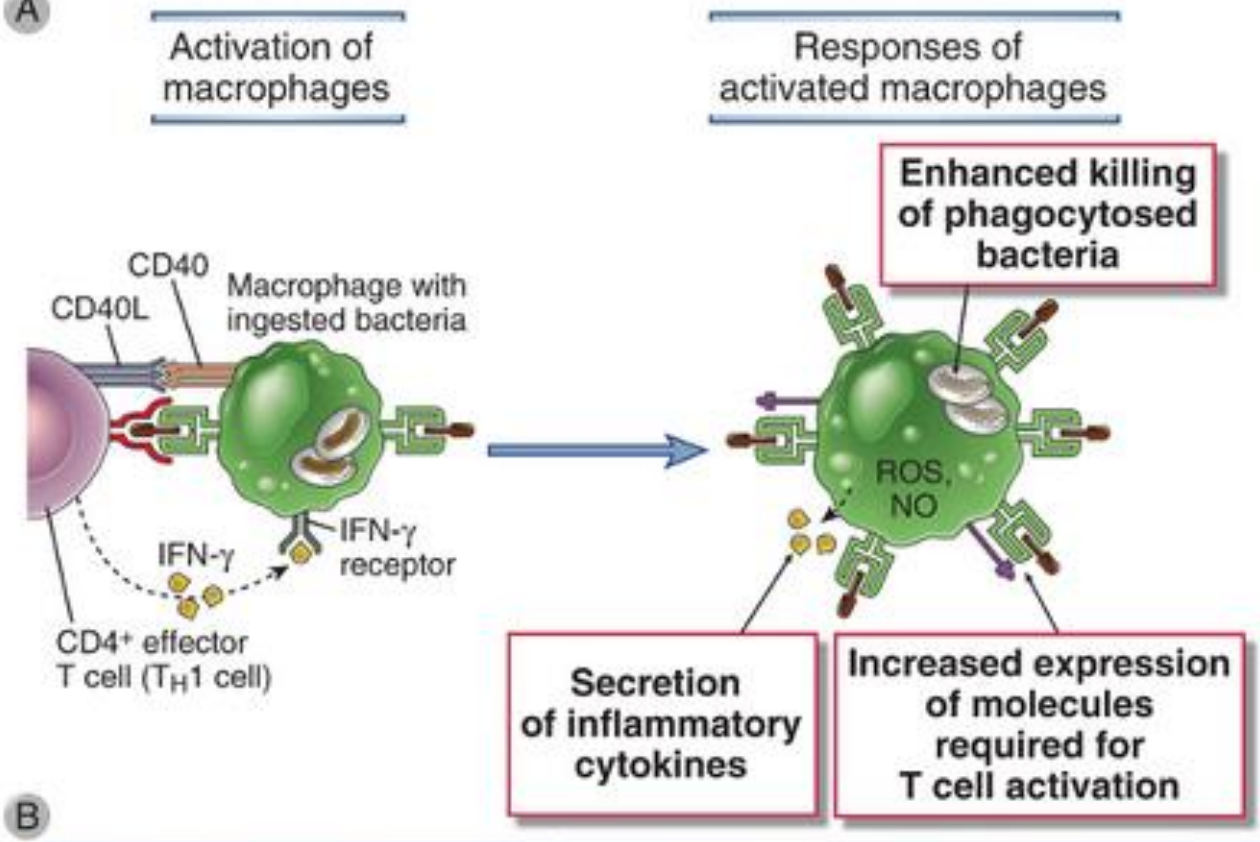

B

Macrophage response	Role in cell-mediated immunity
Production of reactive oxygen species, nitric oxide, increased lysosomal enzymes	Killing of microbes in phagolysosomes (effector function of macrophages)
Secretion of cytokines (TNF, IL-1, IL-12) and chemokines	TNF, IL-1, chemokines: leukocyte recruitment (inflammation) IL-12: T_H1 differentiation, IFN-γ production
Increased expression of B7 costimulators, MHC molecules	Increased T cell activation (amplification of T cell response)

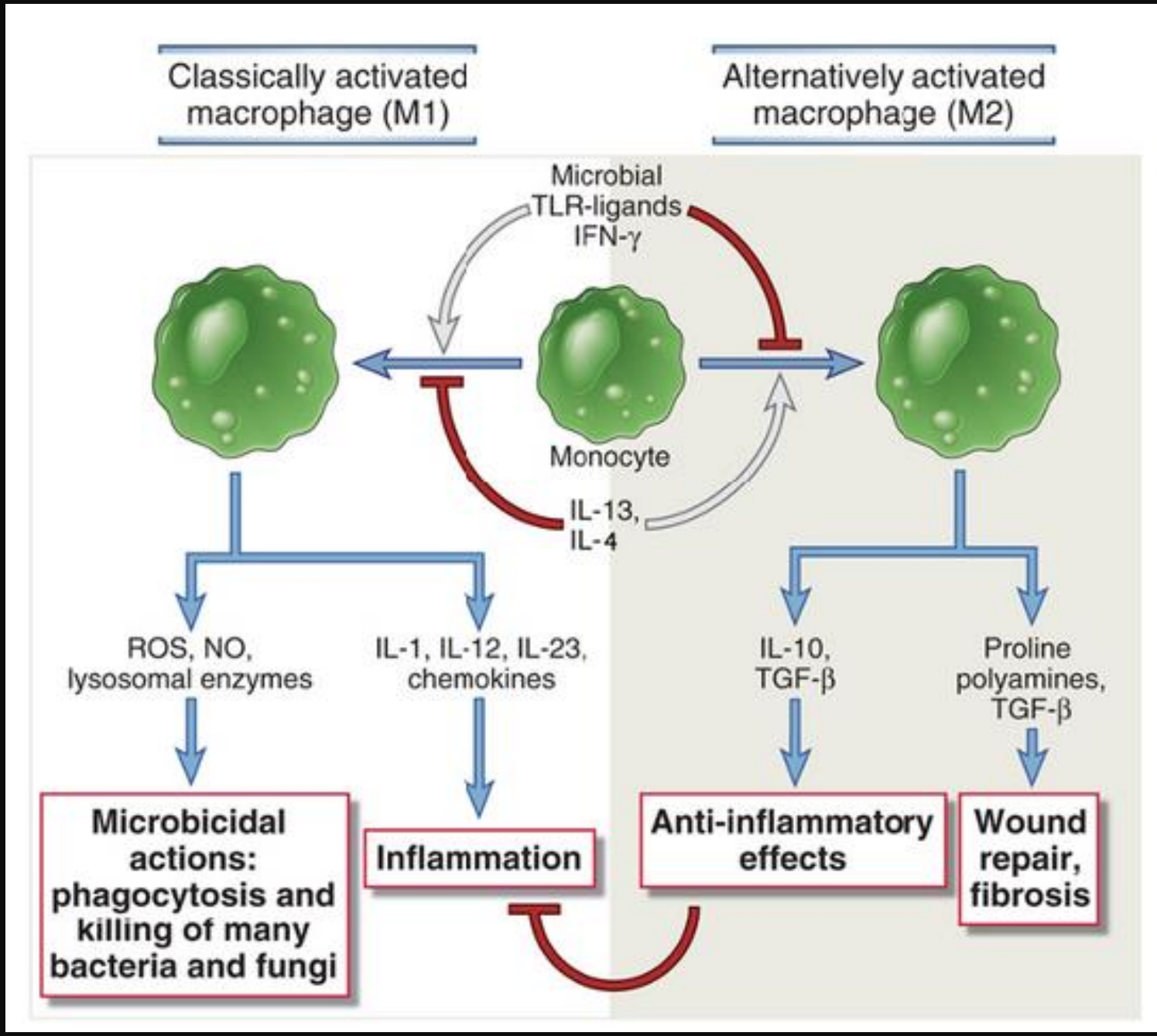
Classically activated macrophage (M1)
Alternatively activated macrophage (M2)
Microbial
TLR-ligands
IFN-γ
Monocyte
IL-13,
IL-4
ROS, NO,
lysosomal enzymes
IL-1, IL-12, IL-23,
chemokines
IL-10,
TGF-β
Proline
polyamines,
TGF-β
Microbicidal actions: phagocytosis and killing of many bacteria and fungi
Inflammation
Anti-inflammatory effects
Wound repair, fibrosis

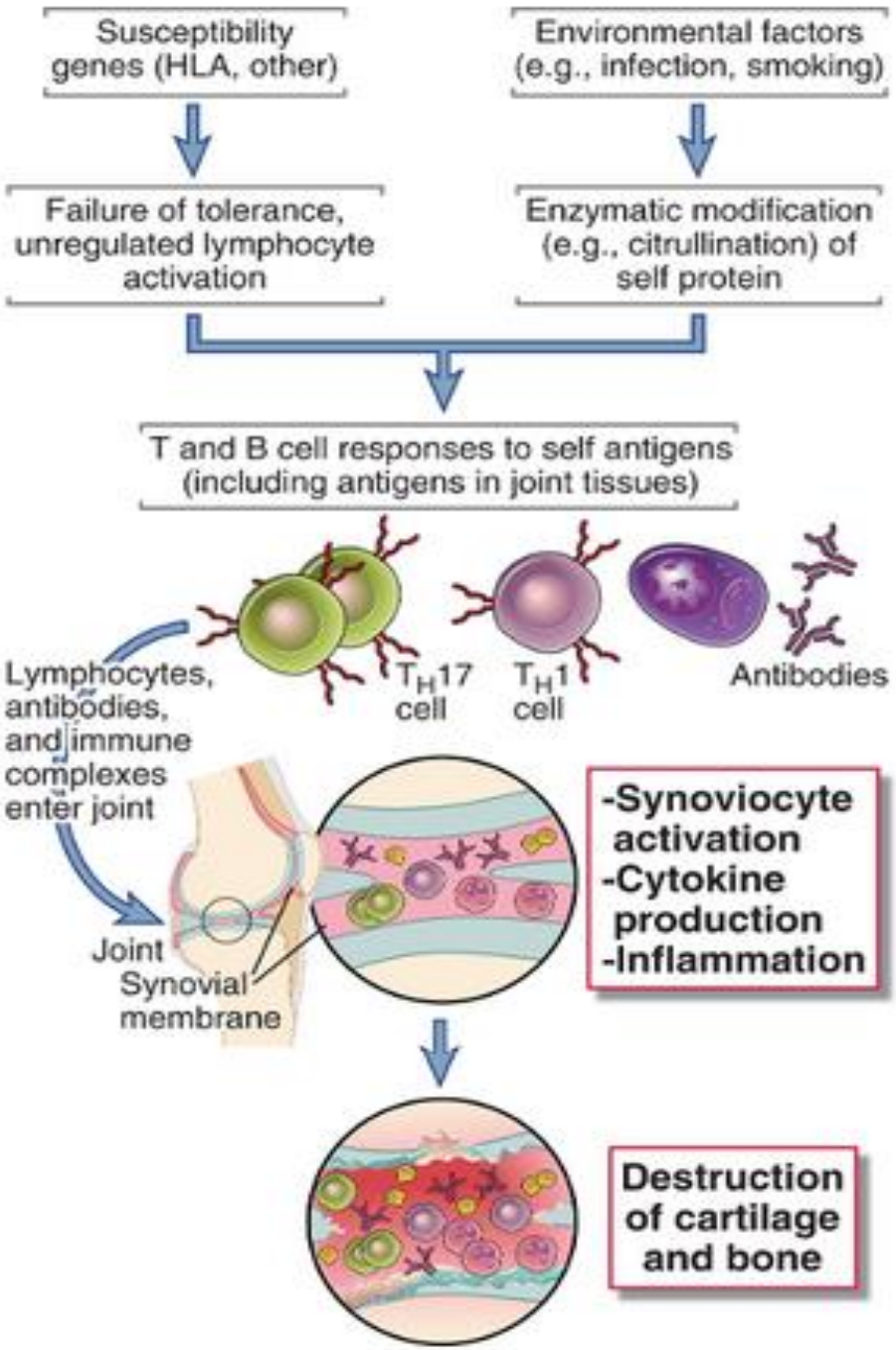

Tipo IV

Antígenos Protéicos

Apresentados

aos Linfócitos T

Th1

Th17

TABLE 18–4 T Cell–Mediated Diseases

Disease	Specificity of Pathogenic T Cells	Principal Mechanisms of Tissue Injury
Rheumatoid arthritis	Collagen? Citrullinated self proteins?	Inflammation mediated by T_H17 (and T_H1?) cytokines Role of antibodies and immune complexes?
Multiple sclerosis	Protein antigens in myelin (e.g., myelin basic protein)	Inflammation mediated by T_H1 and T_H17 cytokines Myelin destruction by activated macrophages
Type 1 diabetes mellitus	Antigens of pancreatic islet β cells (insulin, glutamic acid decarboxylase, others)	T cell–mediated inflammation Destruction of islet cells by CTLs
Inflammatory bowel disease	Enteric bacteria Self antigens?	Inflammation mediated by T_H17 and T_H1 cytokines
Autoimmune myocarditis	Myosin heavy chain protein	CTL-mediated killing of myocardial cells Inflammation mediated by T_H1 cytokines

Examples of human T cell–mediated diseases are listed. In many cases, the specificity of the T cells and the mechanisms of tissue injury are inferred on the basis of the similarity with experimental animal models of the diseases.

Diabetes Tipo I


Willy Gepts (1922-1991)

- Willy Gepts -
- USA – 30.000 novos casos por ano
- HLA – DR3 e HLA-DR4
- Não HLA- Polimorfismo no gene insulina
- Auto-antígenos
  - Anti-insulina
  - Islet cell antigen 512
  - GAD (descarboxilase do ácido glutâmico)
  - Mimetismo molecular – Coxsackie vírus B, reovírus 1b, rubéola
- Experimentalmente a transferência de linfócitos T CD4 ou T CD8 induzem a doença
- Linfócitos B ou anticorpos não!

Gepts W. Pathologic anatomy of the pancreas in juvenile diabetes mellitus. Diabetes 1965;14:619–33

Imunopatologia – Na fase inicial é observado infiltrado inflamatório de linfócitos – macrófagos - INSULITE

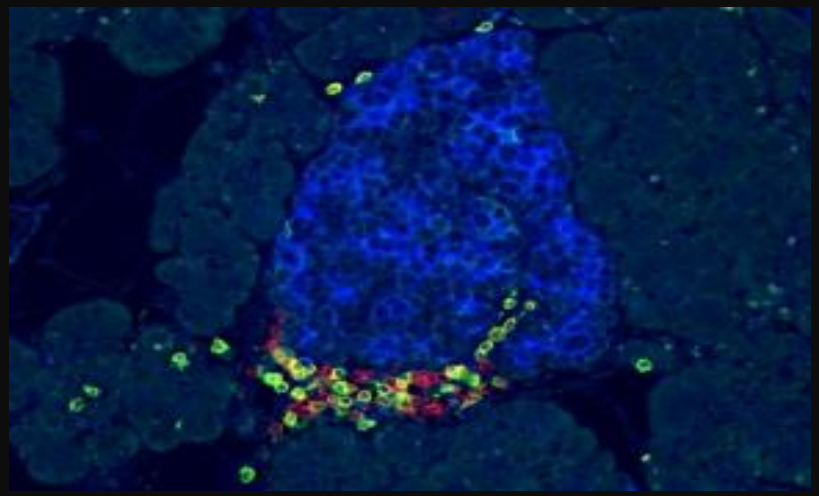

CD3 CD8

Table 1. Classification and observations on types of diabetes mellitus

Type	Characteristic	Clinical comment
Type 1	Autoimmune, previously called juvenile or insulin-dependent diabetes mellitus	Potential association with other autoimmune diseases
Type 2	Polygenic and influenced by environment	Increasing incidence associated with higher life span and western cultural habits
Gestational	Aggressive clinical progress	May persist after pregnancy
Secondary	Side effect of medications or pancreas dysfunction (e.g.; steroids, chronic alcoholism)	Causative disease or medication may also influence ocular and lacrimal function
Genetic	Genetic defects in insulin secretion or action	Potential ocular associated malformations

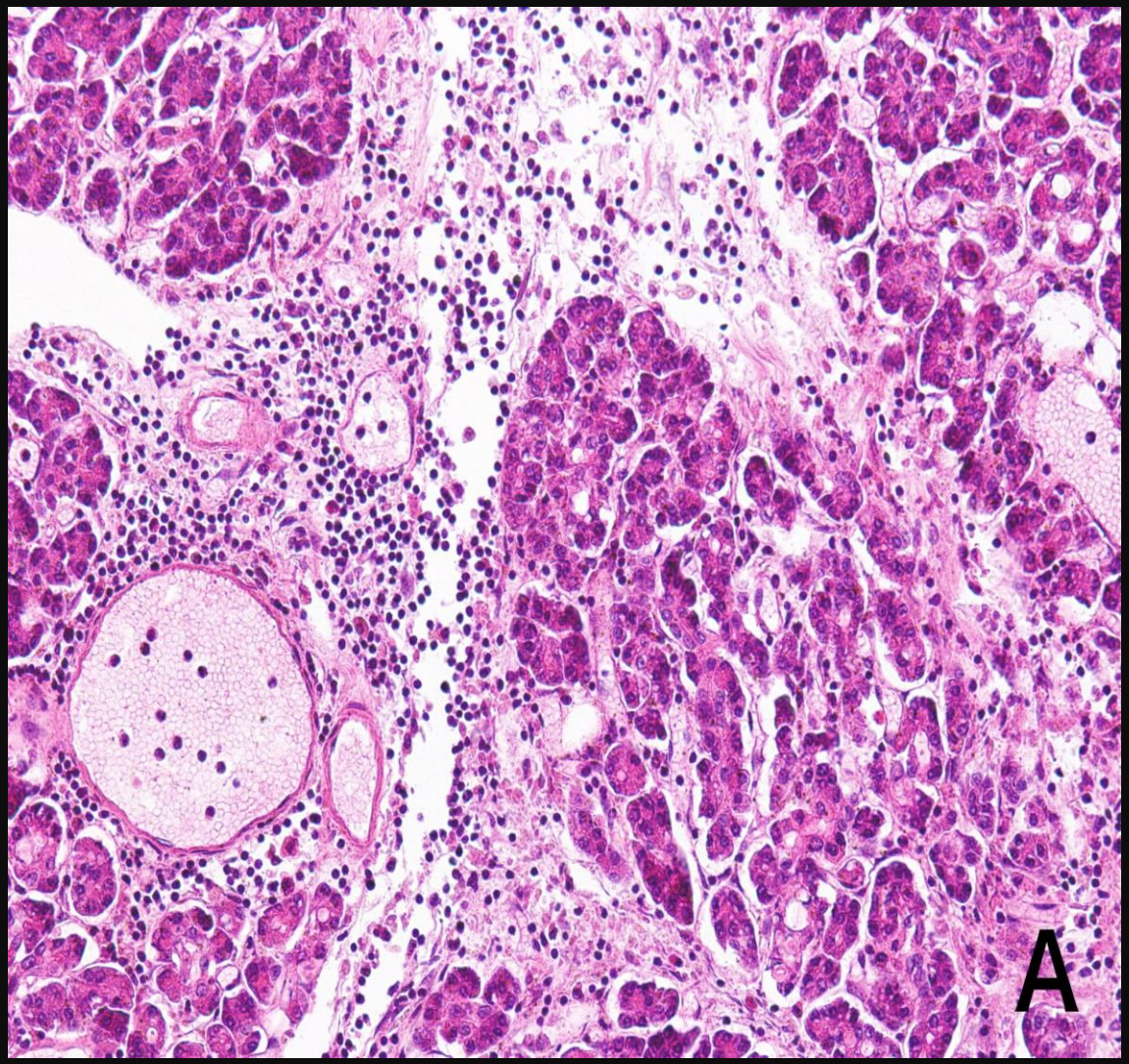

Diabete fulminante

infiltrado inflamatório e fibrose

Imunopatologia – Na fase crônica da doença, devido à ampla destruição das ilhotes e redução do Ag, há uma grande regressão do infiltrado inflamatório

Ilhotas Controle

Paciente Diabético
19 anos evolução

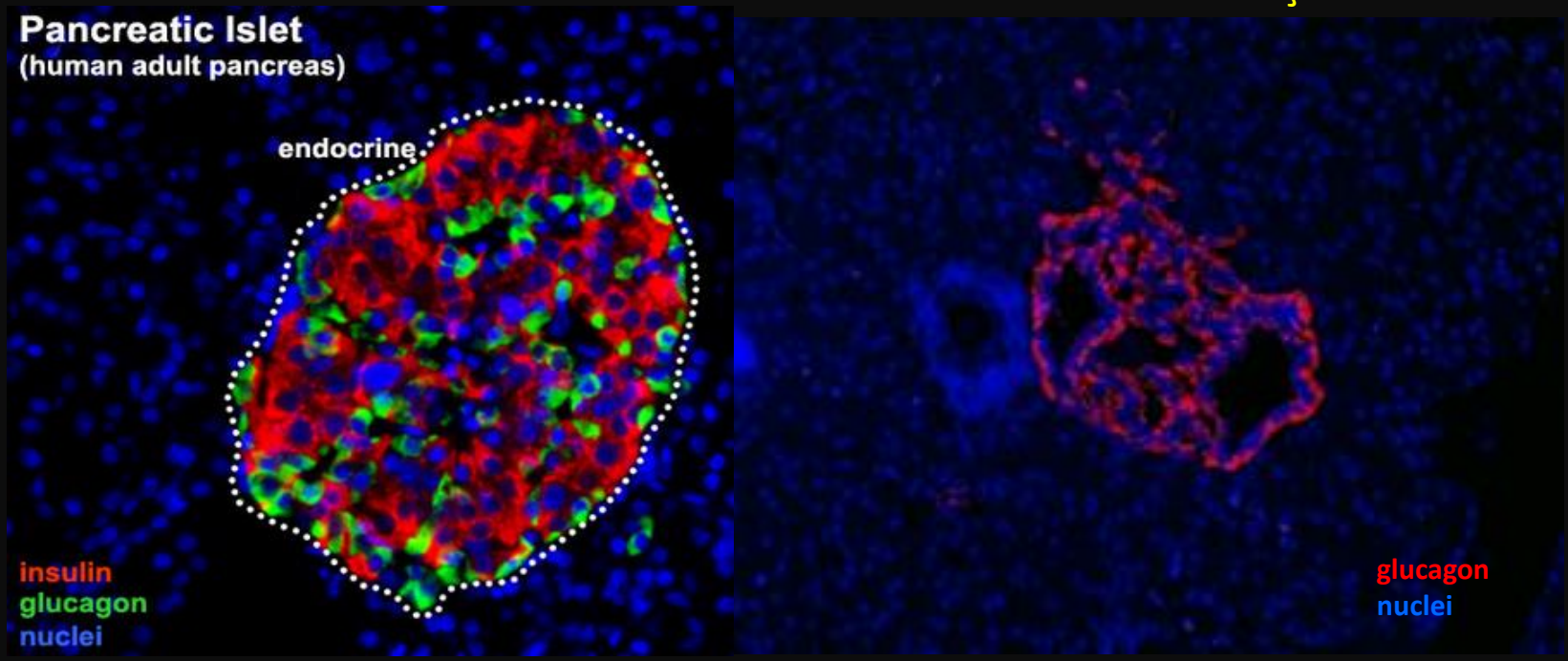

While >70% of young patients with acute onset of the disease show insulitis (in 5-10% of their islets), the lesion is present in only 4% of patients one year after the diagnosis is made. The inflammation disappears together with the remaining beta cells, leaving small islets that are devoid of any insulin-positivity⁻

nature materials

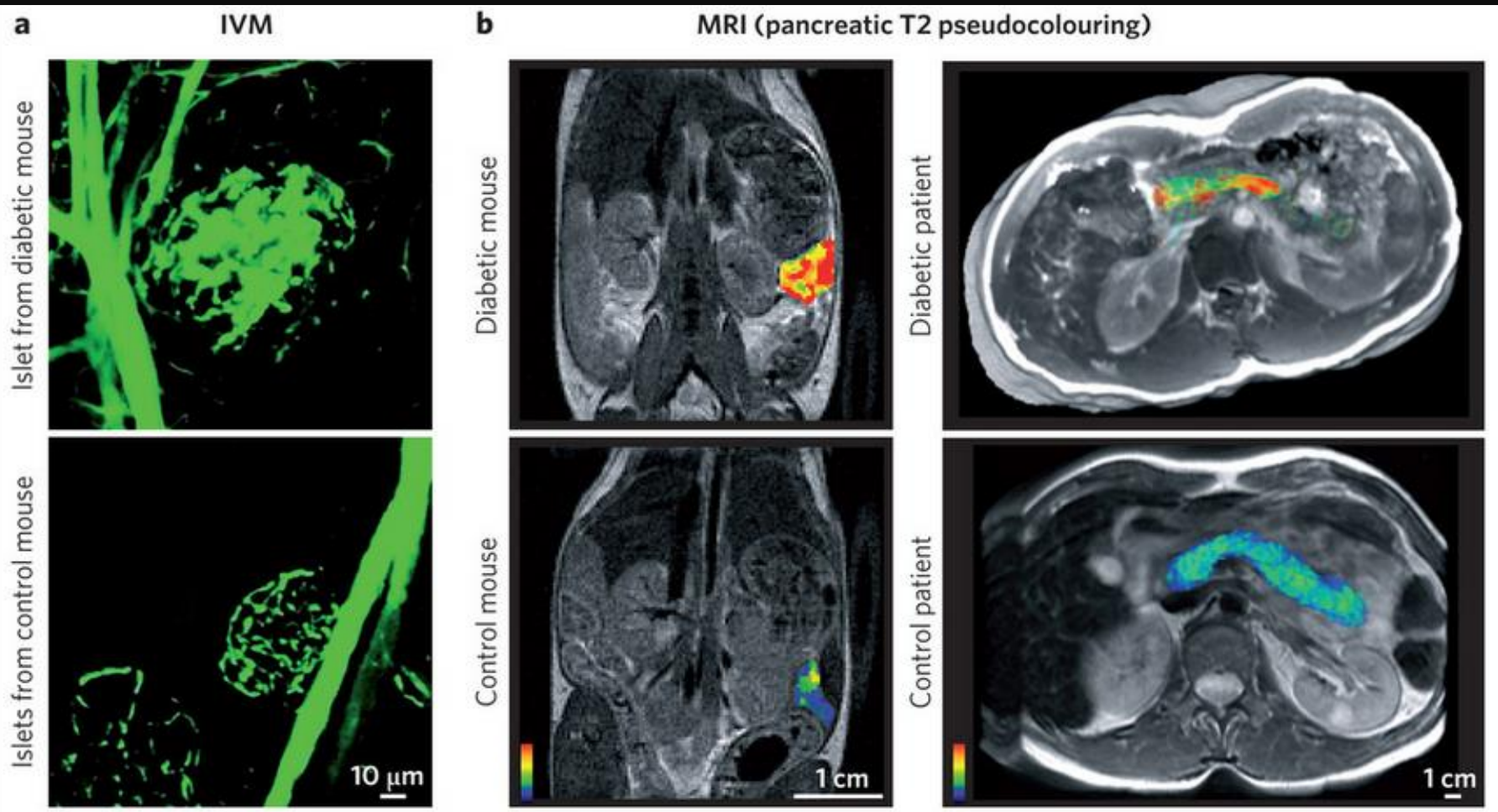

a, During type 1 diabetes development, islets of Langerhans contain inflammatory cells (insulitis) and show increased microvascularity and permeability, shown here by intravital imaging (IVM) during the perfusion phase of a dextran nanoparticle (crosslinked iron oxide nanoparticles labelled with fluorescein isothiocyanate)[158]. At later phases, nanoparticles accumulate in macrophages in insulitis islets. **b**, Changes in T2, indicative of nanoparticle accumulation in insulitis, are pseudocoloured and superimposed onto T1 images. In both mice[159] and human patients[160], there is a clear difference between type 1 diabetes (top) and normal individuals (bottom).

Tireoidites – Doença de Graves

- HLA – DR3, HLA – D8
- Auto-antígenos
  - Receptor TSH – porção extracelular, porém anticorpos contra as porções transmembrana já foram detectados
  - Anti-TPO (Tireoperoxidase) – não costumam ser patogênicos
- Mimetismo molecular – Vírus, *Yersinia enterocolítica*
- Resposta Th1-Th17 – citocinas pró-inflamatórias IL-1, IL-4, IL-5, IL-8, IL-12, IFN-γ, TNF-α...

Doença de Graves

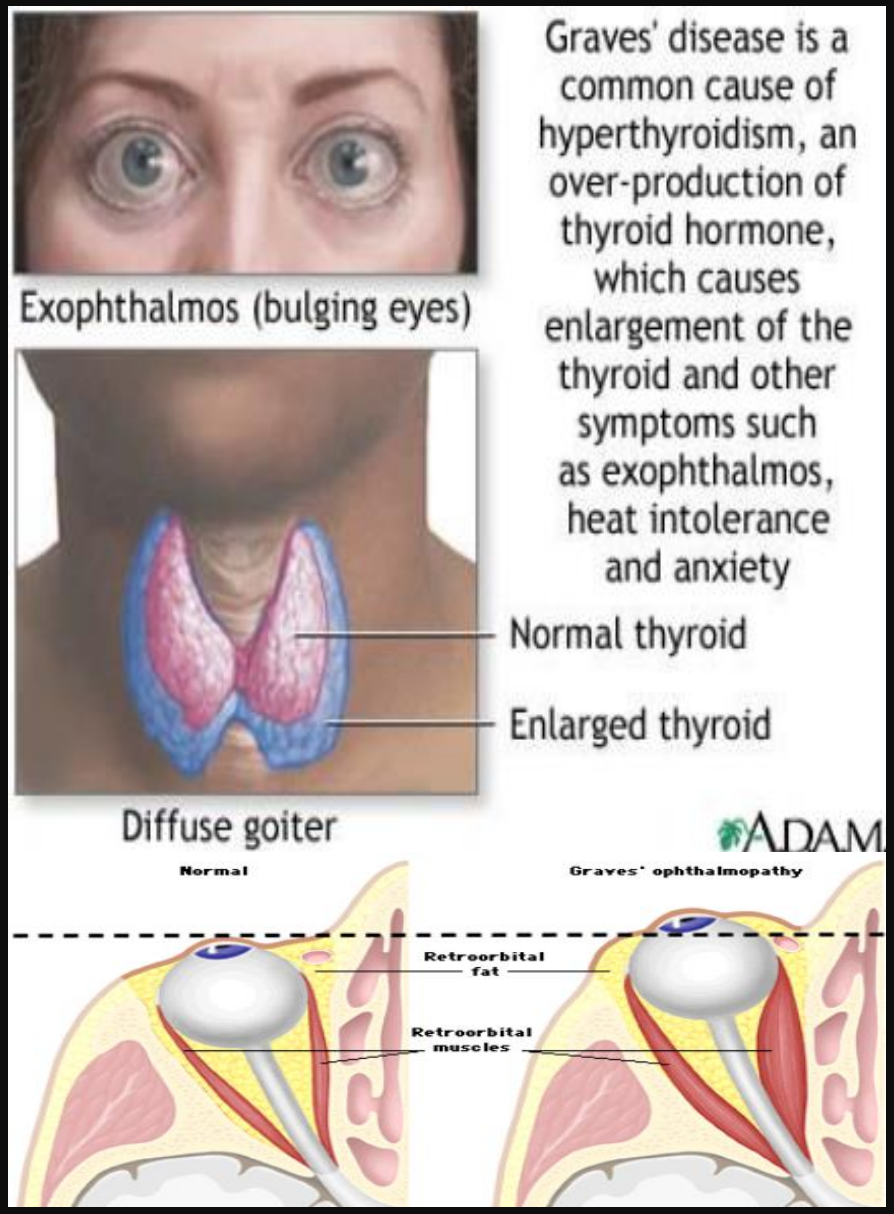

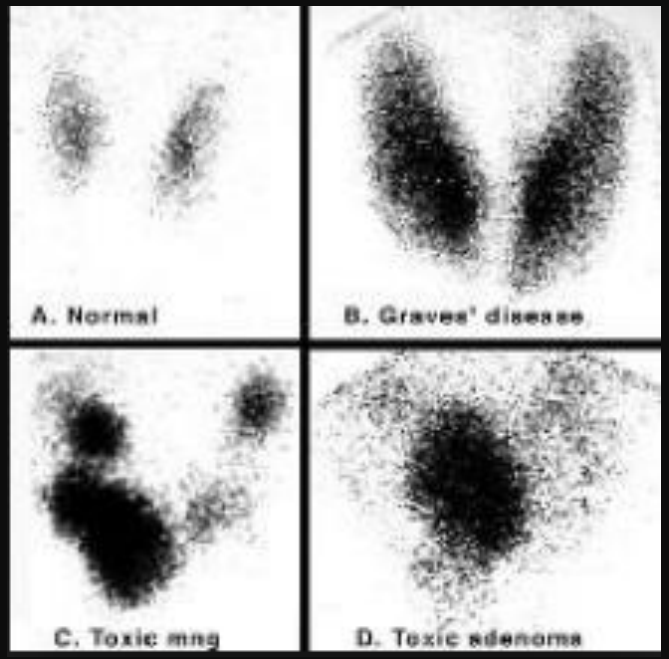

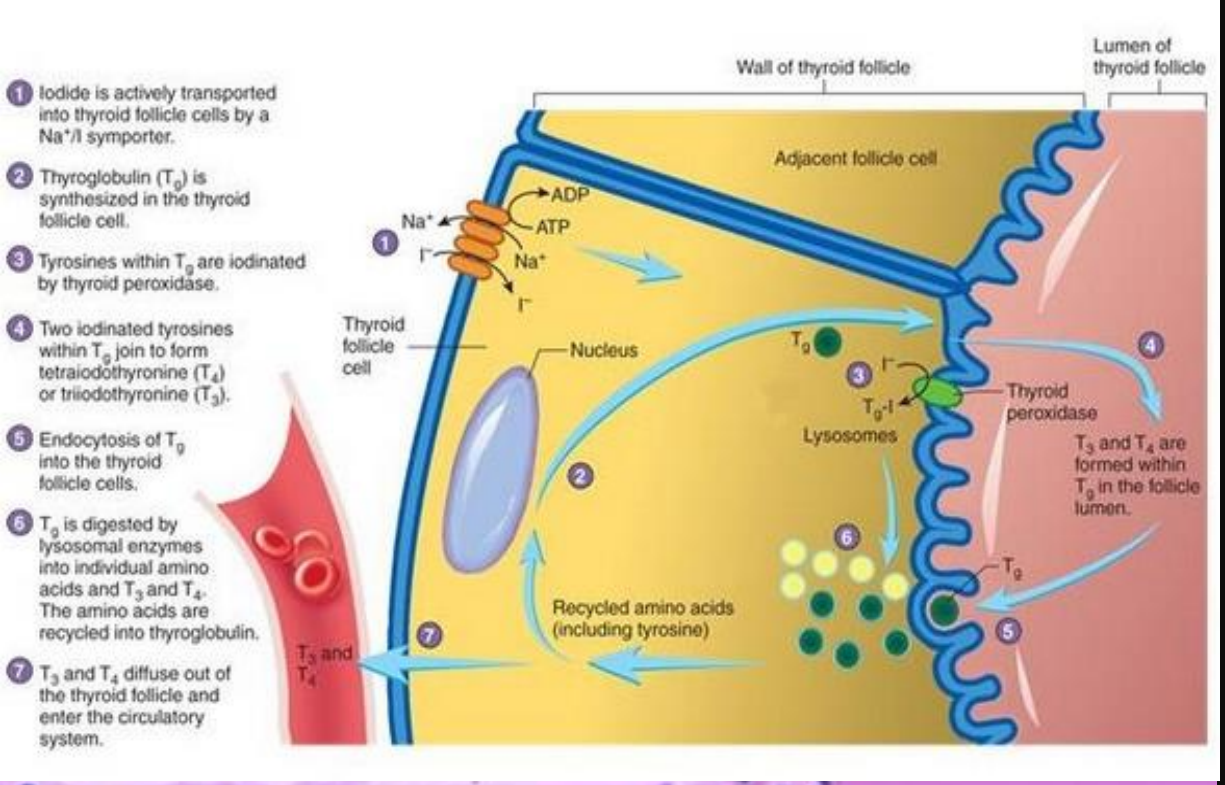

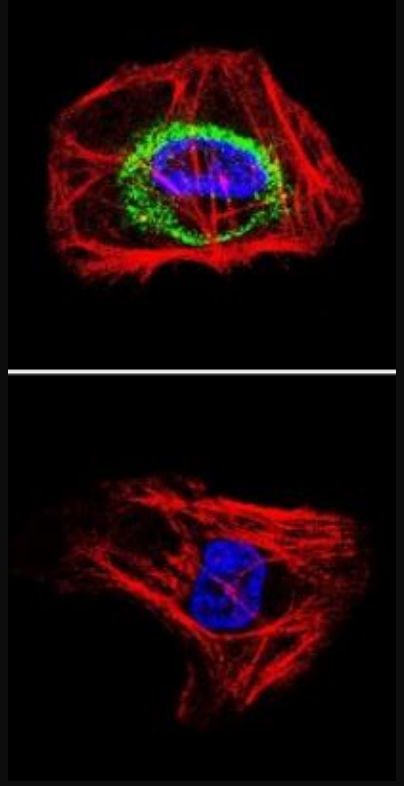

TSHR
In vitro

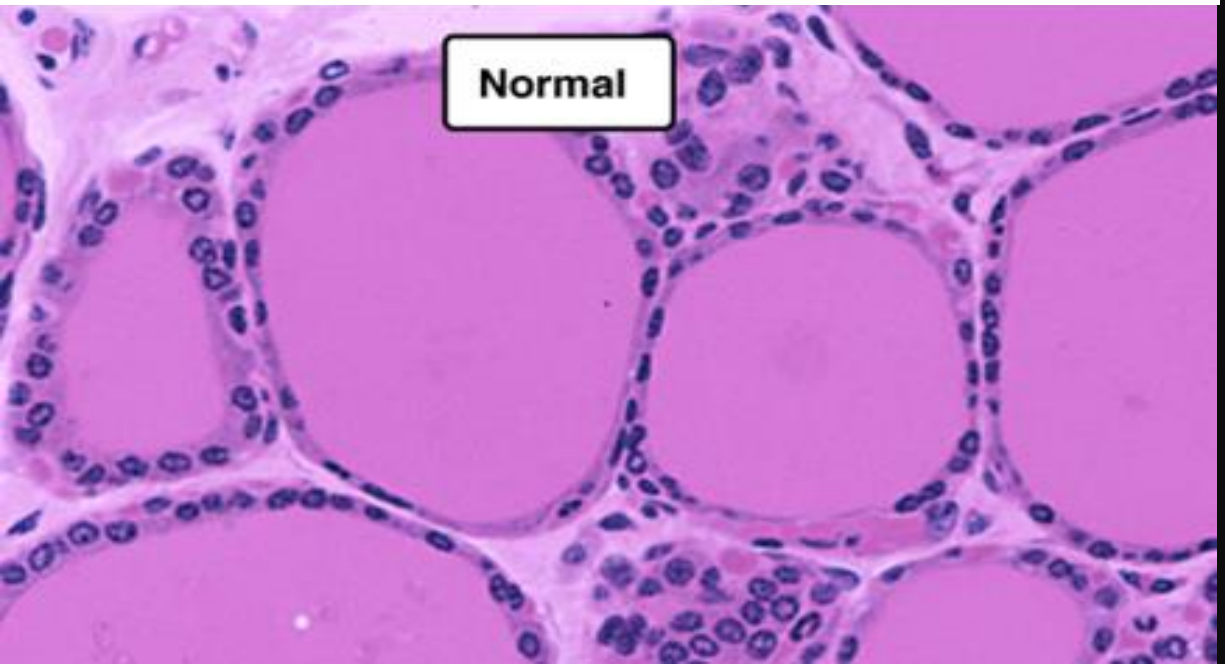

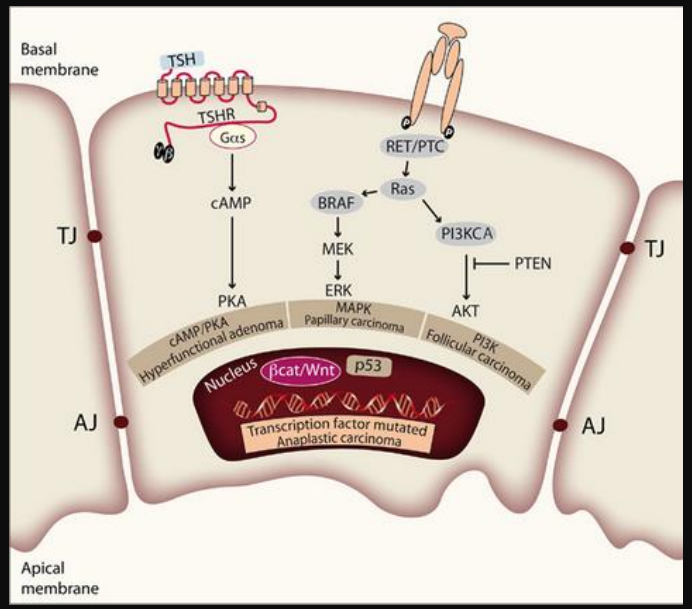

Fisiopatogenia

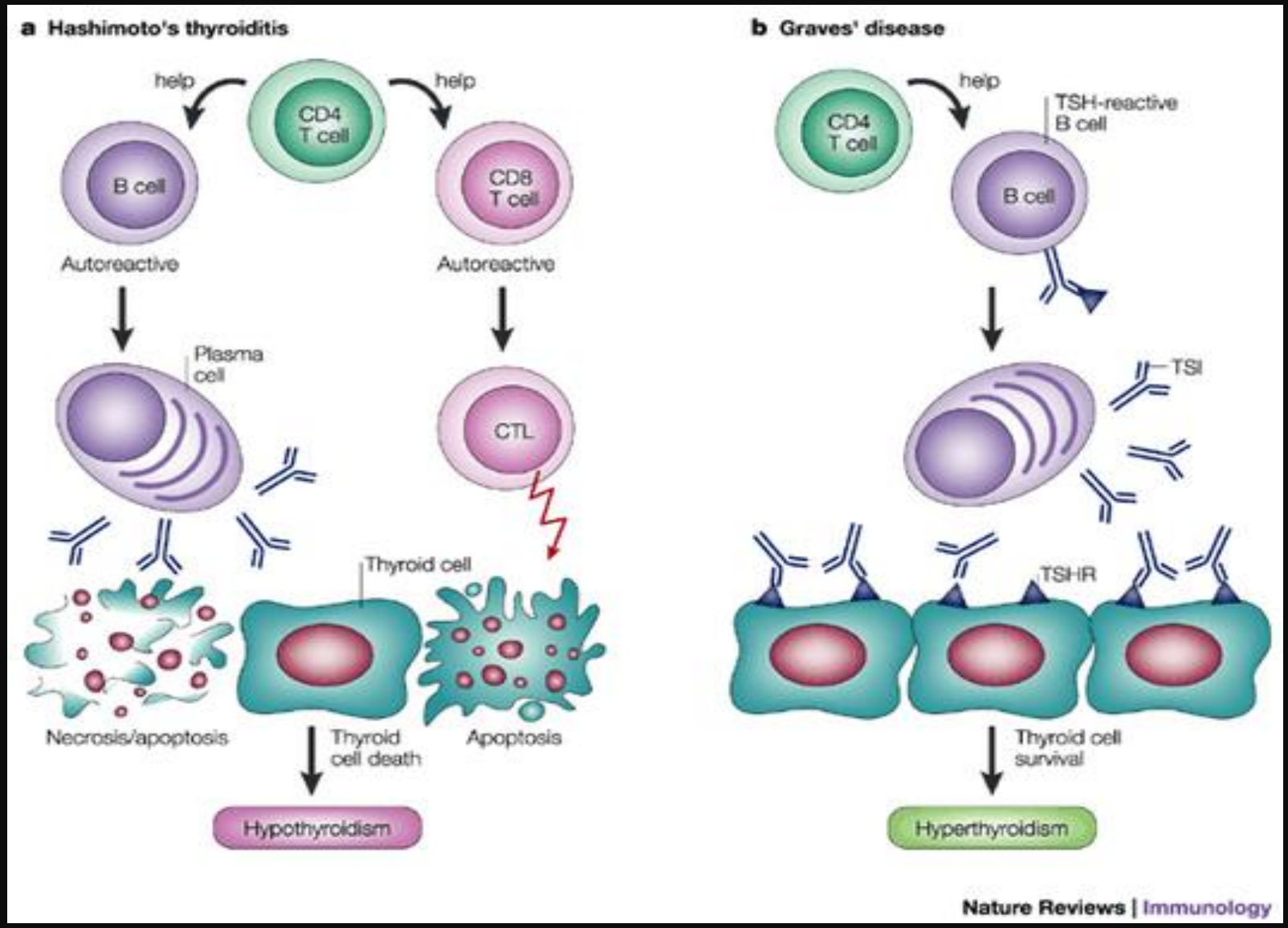

Histopatologia

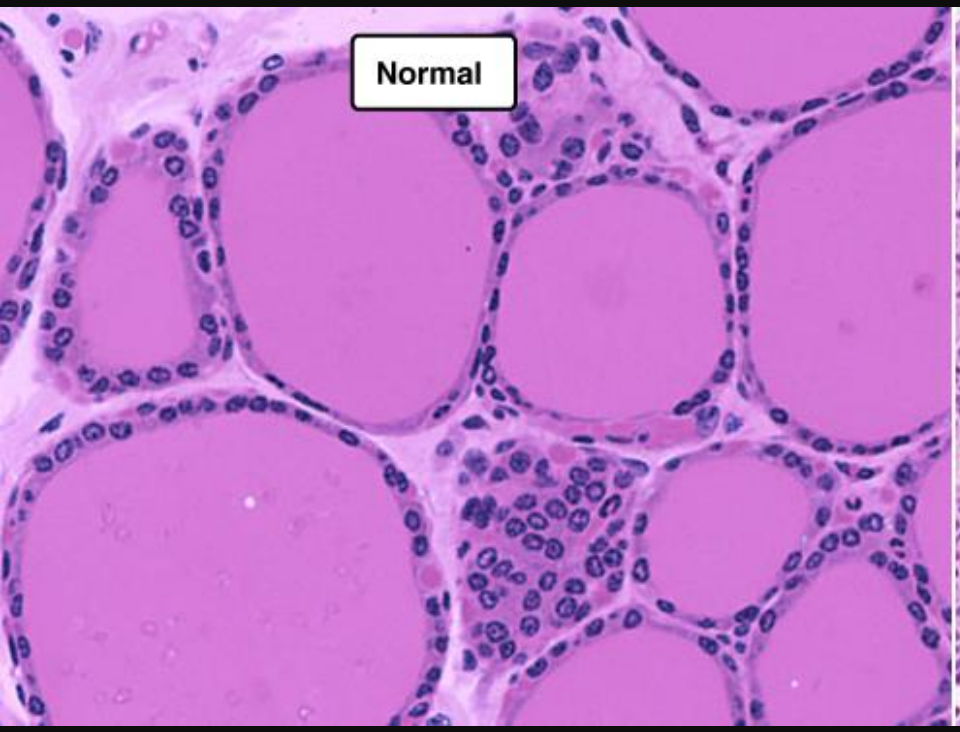

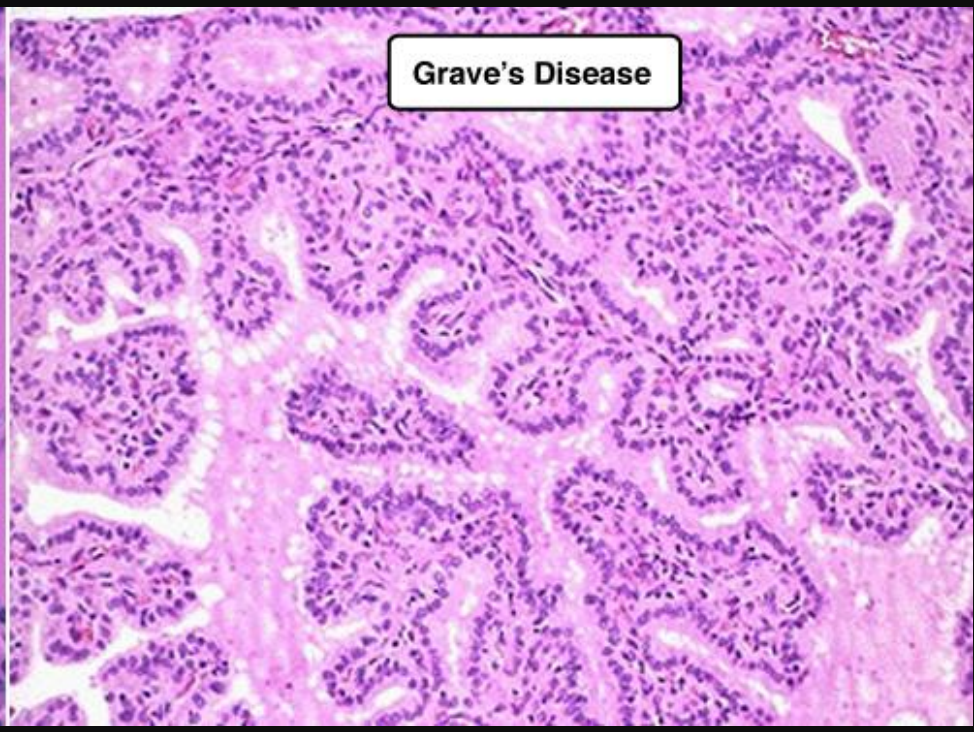

Paciente

Hipertireoideo

Magro

Bócio

Exolftalmia

Ansioso

Distúrbios do sono

Metabolismo acelarado

Tireoidite de Hashimoto – Tireoidite Crônica Linfocítica

- 3,5 – 1000 mulheres – 14 / 1000 após 60 anos de idade
- Comum doença se iniciar após a puberdade ou gravidez
- HLA – DR3, HLA – DR4, HLA – DR5
- Antígenos
  - Anti-tireoglubulina – 100% pacientes
  - Anti-TPO (tireoperoxidase)
  - Anti-TSH – 10-20% pacientes (bloqueador)

- Infiltrado de células Th1 – IFN-γ
- Células T CD8 citotóxicas também estão presentes

Histopatologia

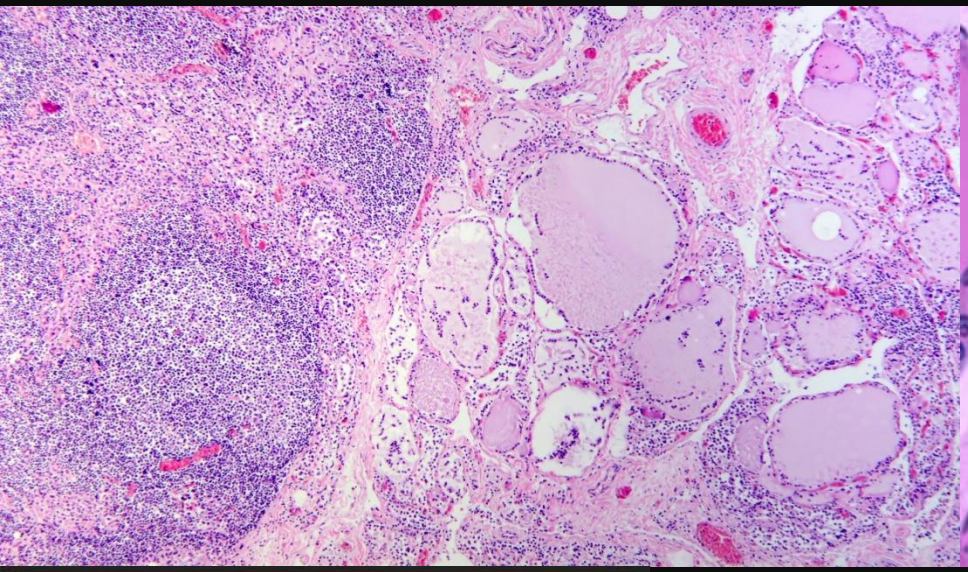

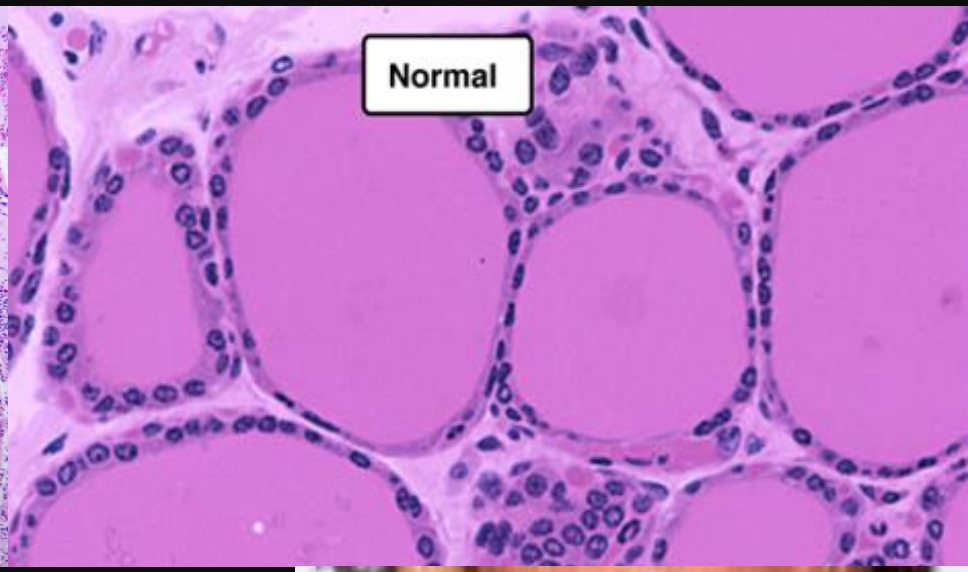

Hipotireoideo
Metabolismo Lento
Obeso

Hurtle Cells
Células foliculares em degeneração
Marcação eosinofílica
Iniciar nódulos tumorais

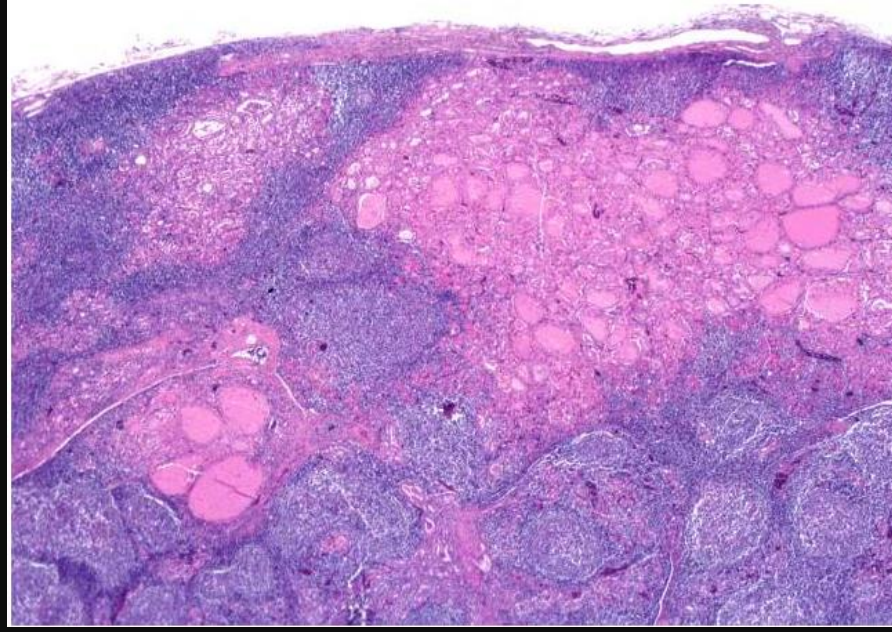

Formação de Centros Germinativos

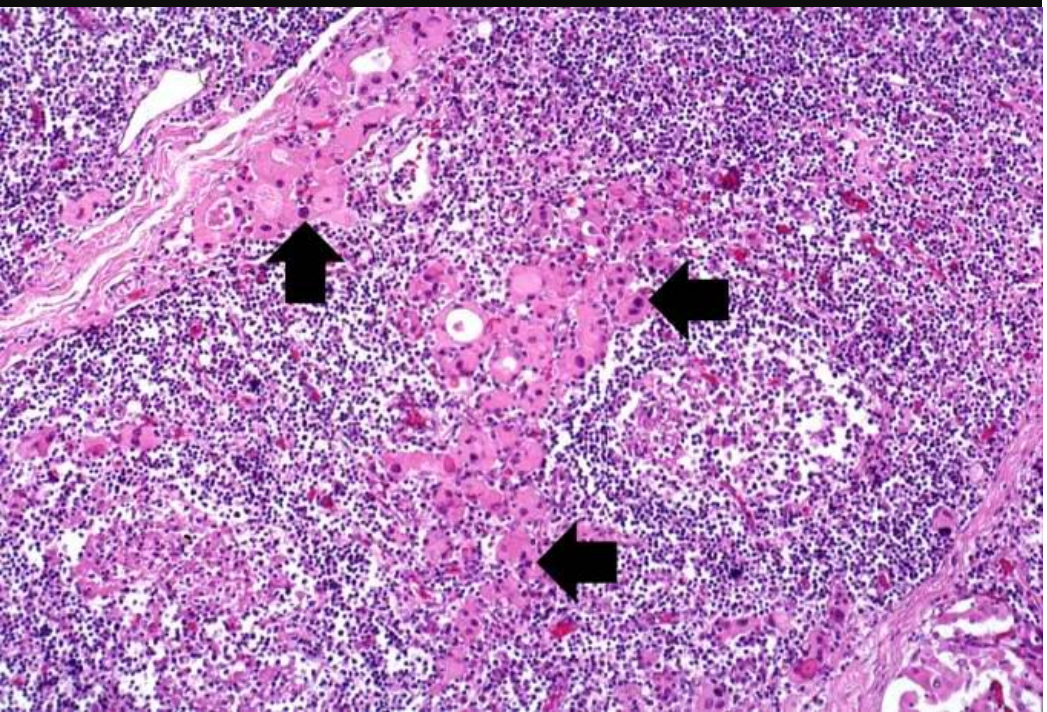

Células Imunes Infilltrantes do SNC são Alvos de Neurotransmissores

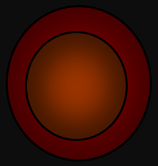

CD4

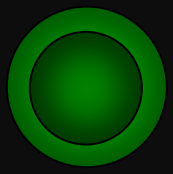

CD8

M φ

DCs

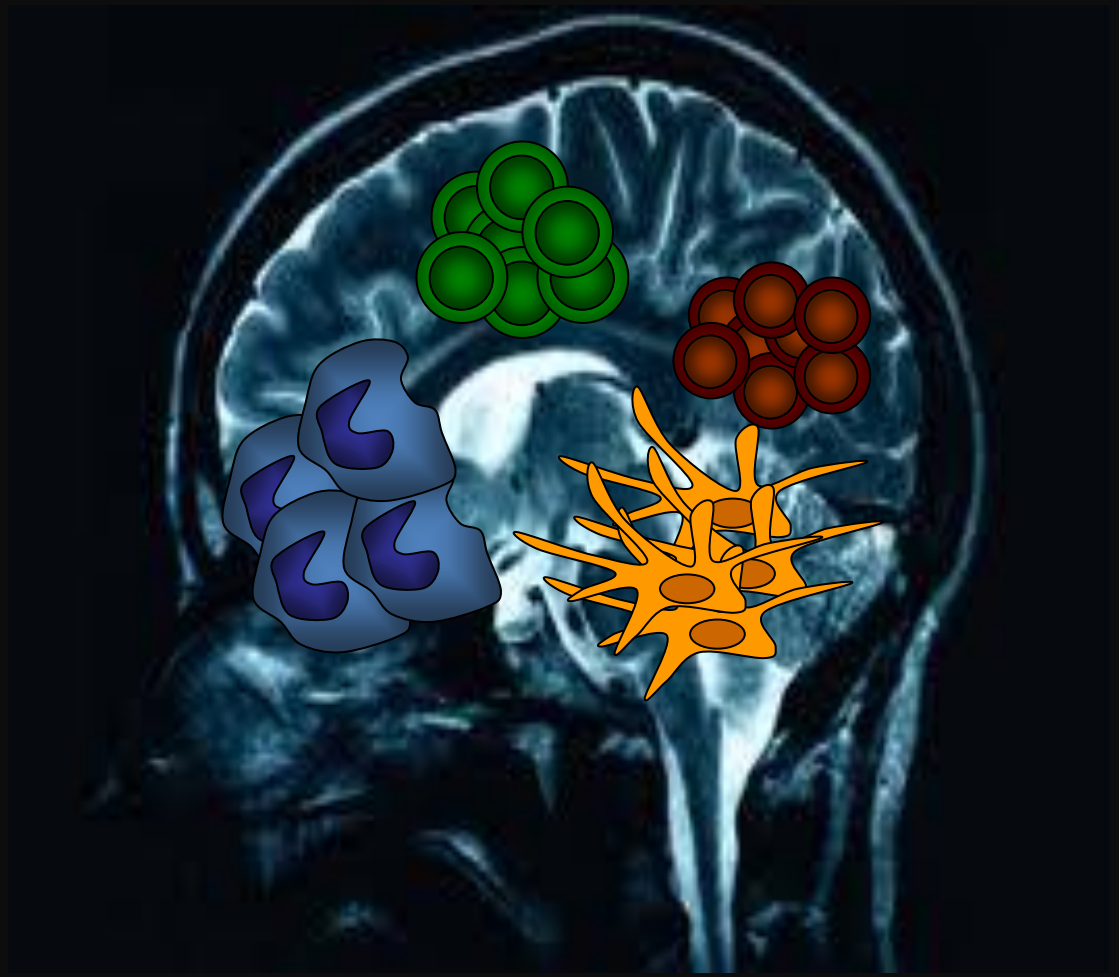

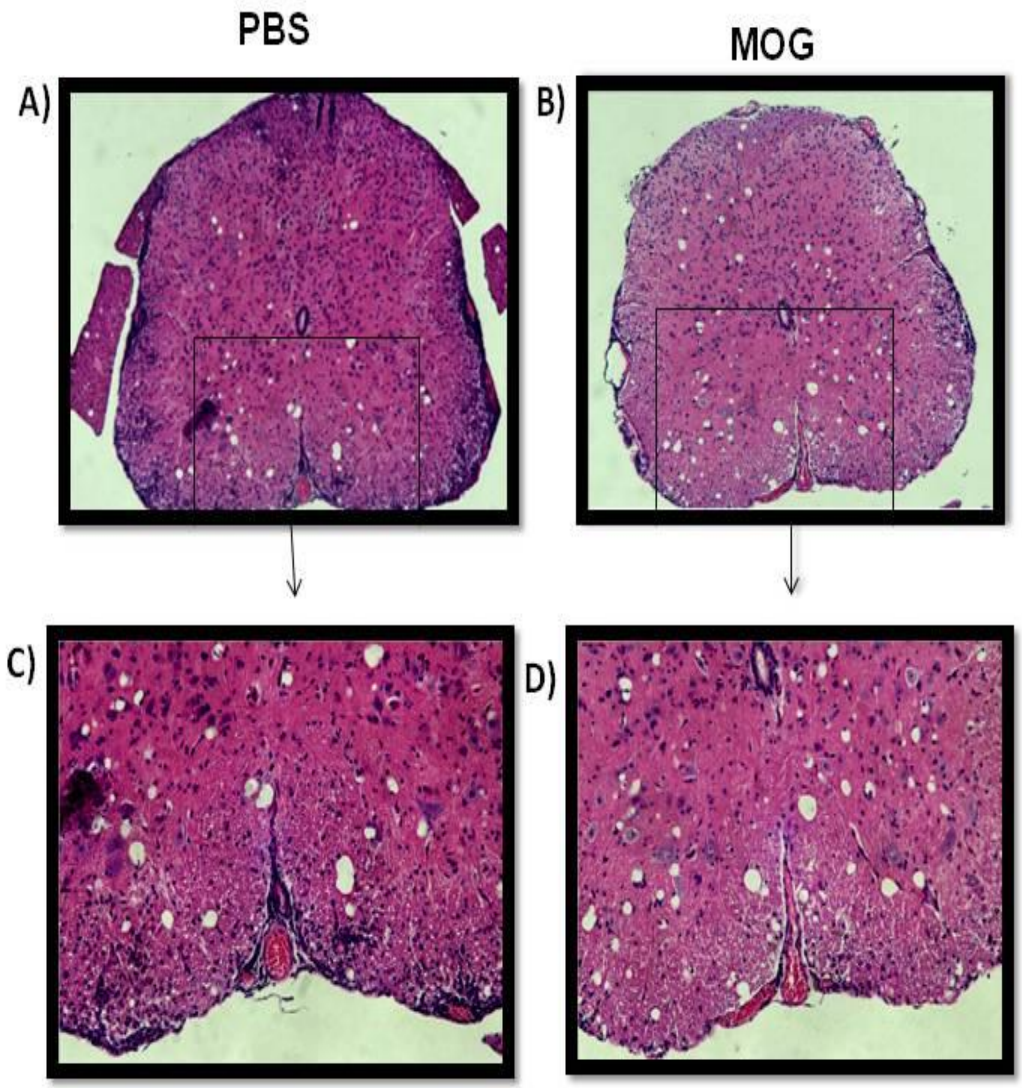

Encefalomielite Experimental Auto-imuneEAE

Modelo Murino para Estudo da Esclerose Múltipla

Ativação do Sistema Imune

Características
Infiltrado inflamatório perivascular
Gliose, Desmielinização,
Lesão axonal e morte neuronal

Utilizando este Modelo
4 Linhas de Pesquisa Principais

1) Tolerância Oral

2) Papel das Células da Microglia

3) Tratamento com MSCs Humanas

4) Papel do neurotransmissor Glutamato como imunomodulador.

Encefalomielite Experimental Auto-imune

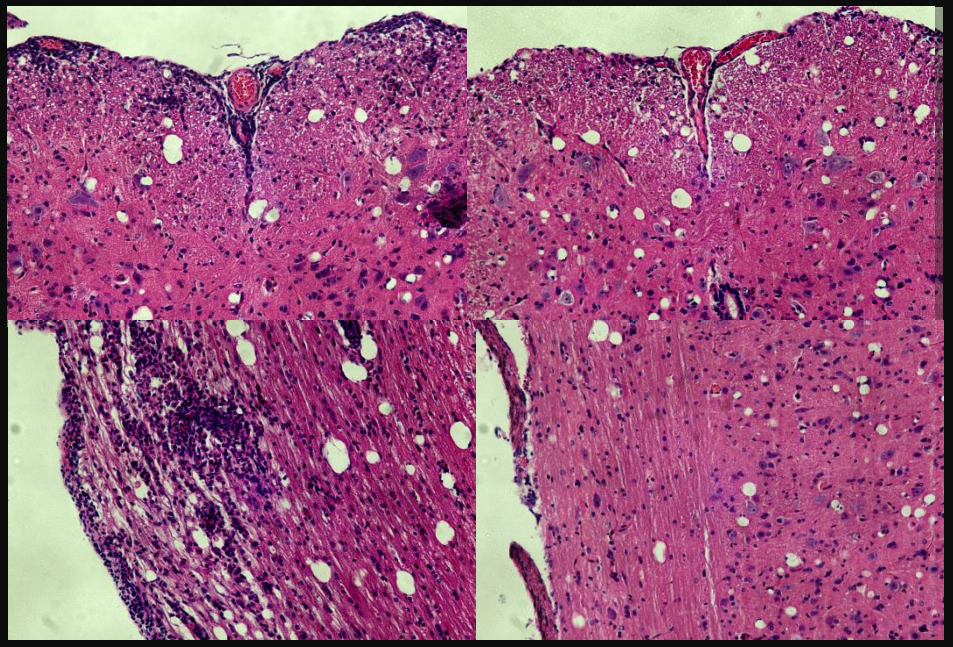

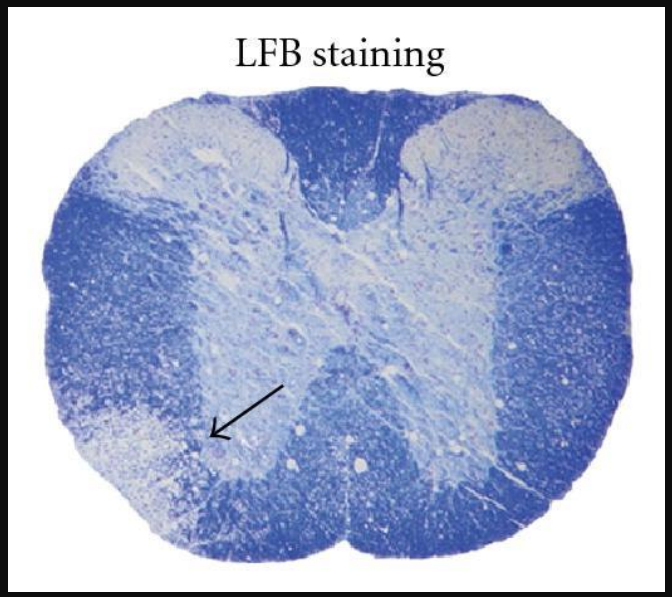

Modelo Murino para Estudo da Esclerose Múltipla

Características

Infiltrado inflamatório
Macrófagos, T CD4, TCD8, DCs

Ativação das Células Residentes

Gliose, Ativação de Células da Microglia
Desmielinização,
Lesão Axonal e Morte Neuronal

Utilizando este Modelo

1) Papel das Células da Microglia
2) Tratamento com MSCs Humanas
3) Papel do neurotransmissor Glutamato como imunomodulador.

Lesões no Sistema Nervoso Central

- Placas Peri-ventriculares (Desmielinização)

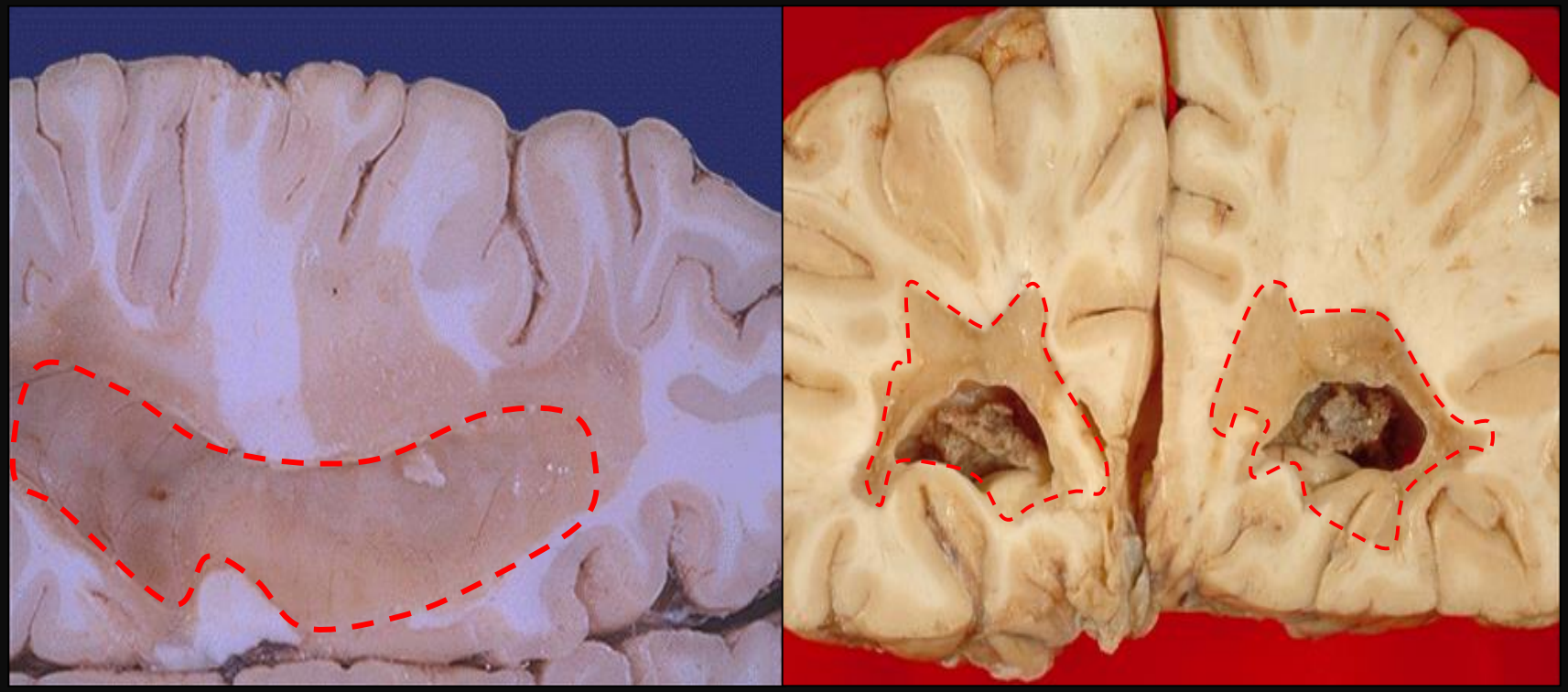

Camundongos com EAE

Esclerose Múltipla

- Inflamação do SNC
  - Infiltrado Inflamatório
  - Gliose
  - Desmielinização
  - Morte neuronal
  - Lesões predominantemente perivasculares

- Progressiva e Remissão
- Secundária progressiva
- Primária progressiva
- Pico e remissão

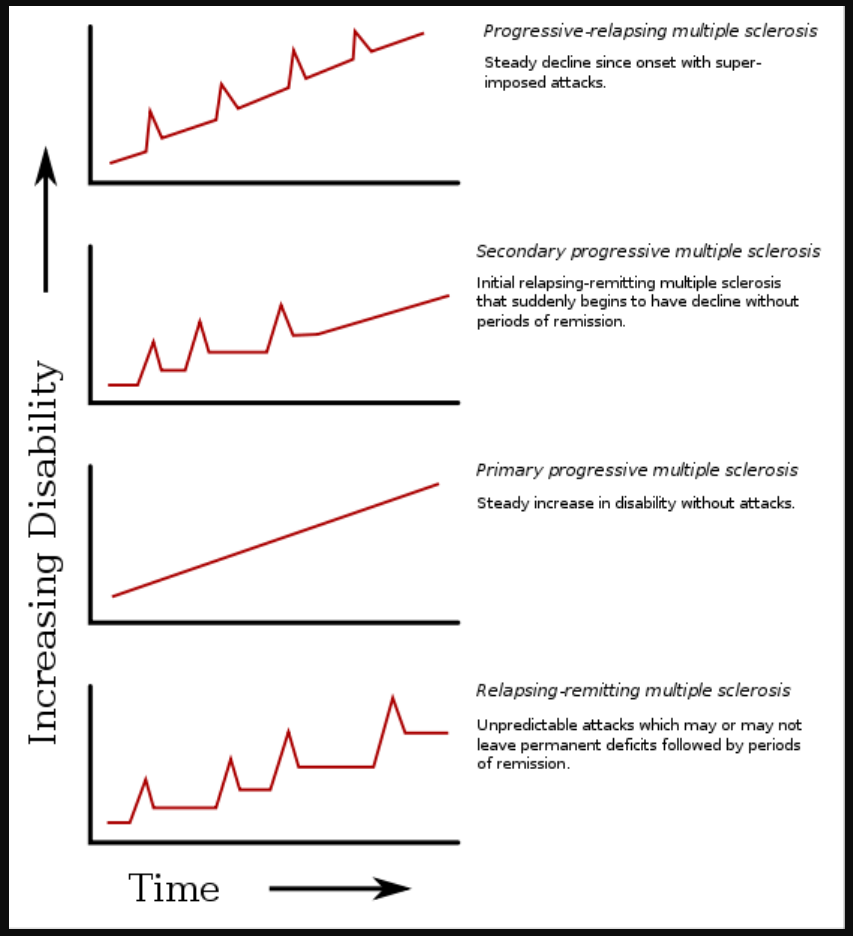

Lublin FD, Reingold SC (April 1996). "Defining the clinical course of multiple sclerosis: results of an international survey. National Multiple Sclerosis Society (USA) Advisory Committee on Clinical Trials of New Agents in Multiple Sclerosis". *Neurology* **46** (4): 907–11. PMID 8780061.

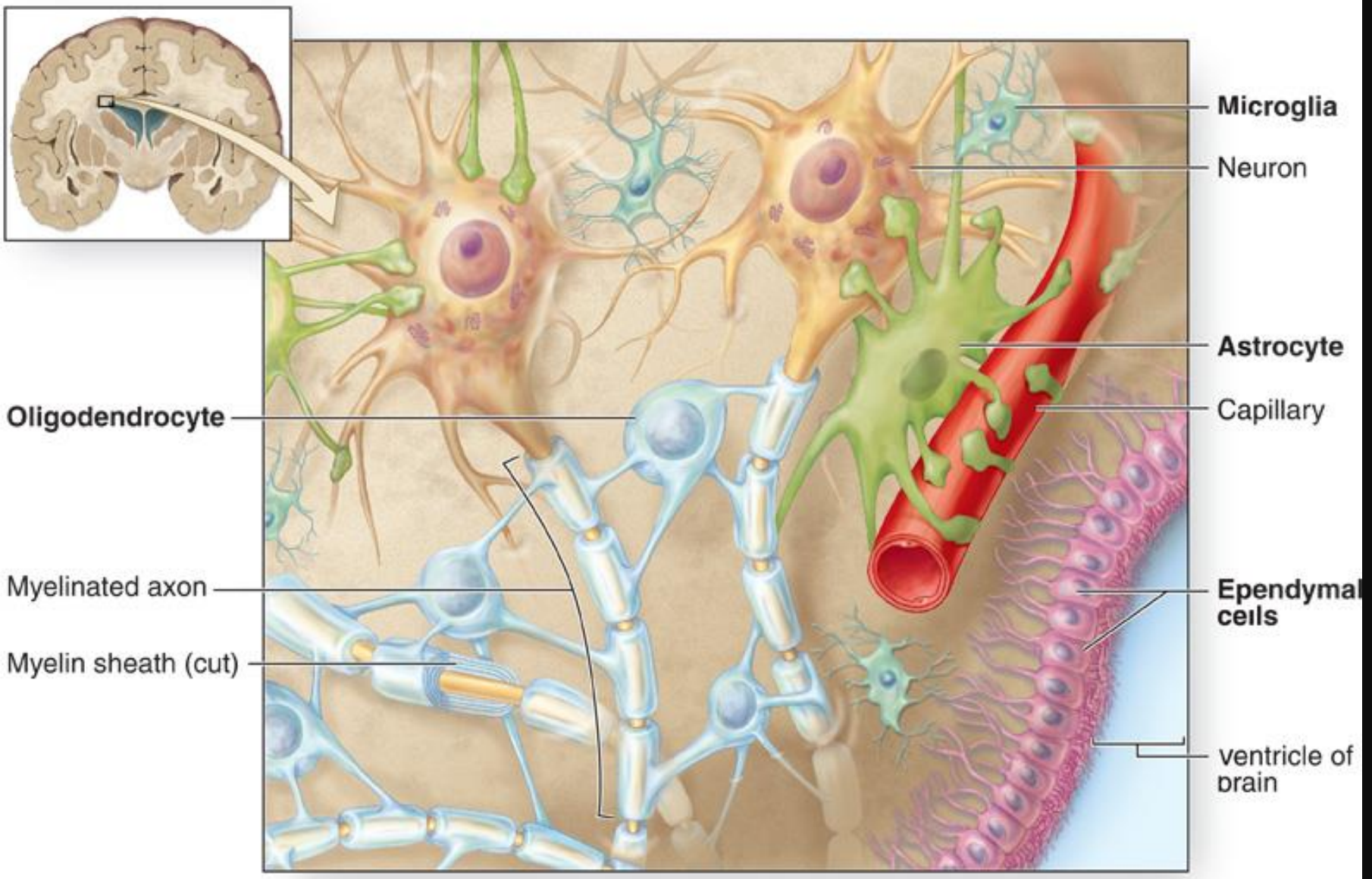

O Papel do Sistema Imune

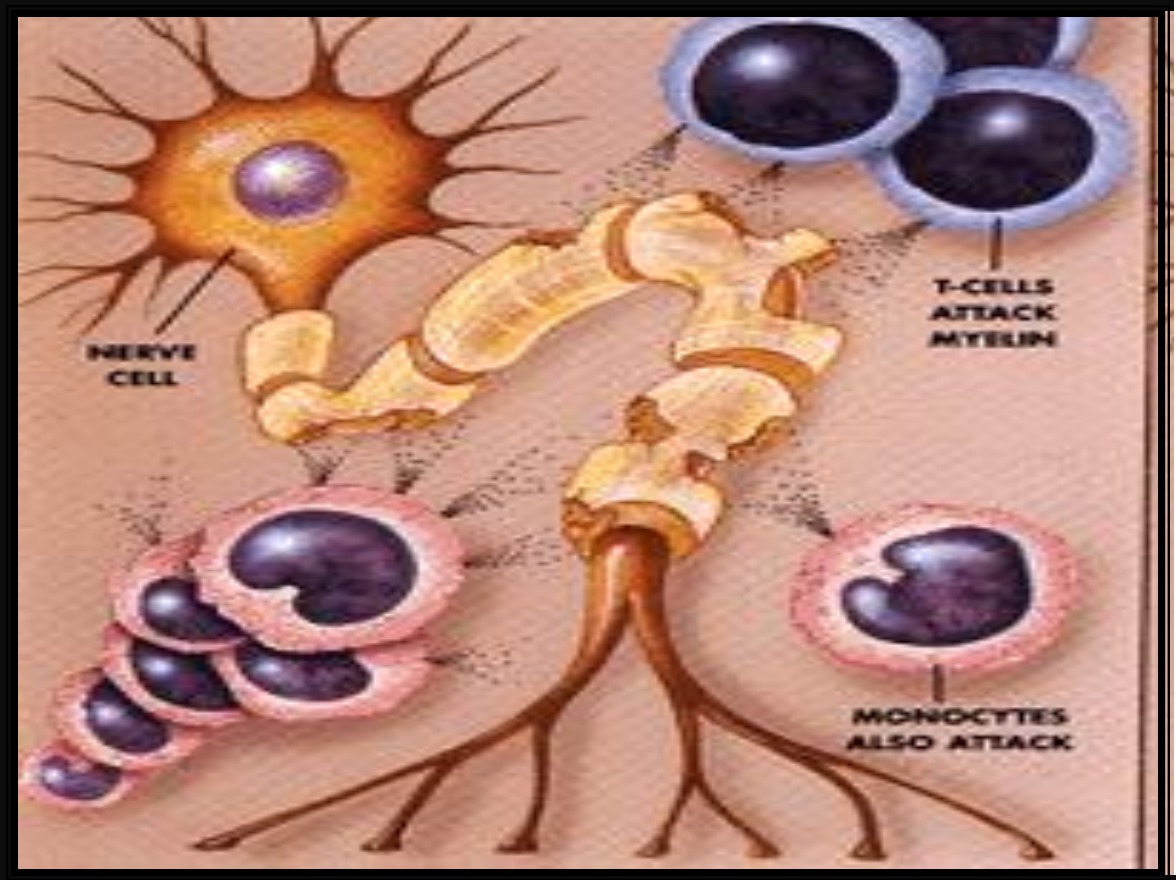

Citocinas
IL-1, IL-6, IL-12
IL-17, IL-23, IFN-γ

NO
ROIs

MMP-3
MMP-9

Granzimas

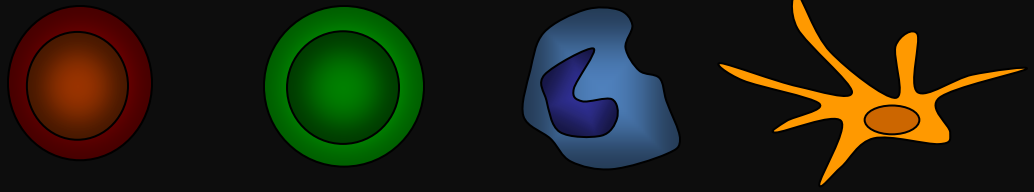

CD4 CD8 M φ **Células Dendríticas**

IDO
Glutamato

Abordagens Terapêuticas

TABLE 18–5 Examples of Cytokine Antagonists in Clinical Use or Trials

Cytokine or Receptor Targeted	Predicted Biologic Effects Of Antagonist	Clinical Indications
TNF	Inhibits leukocyte migration into sites of inflammation	Rheumatoid arthritis, psoriasis, inflammatory bowel disease
IL-1	Inhibits leukocyte migration into sites of inflammation	Rare autoinflammatory syndromes, severe gout, rheumatoid arthritis
IL-6 and IL-6 receptor	Inhibits synthesis of acute-phase proteins, antibody responses?	Juvenile idiopathic arthritis, rheumatoid arthritis
IL-17	Inhibits leukocyte recruitment into sites of inflammation	Rheumatoid arthritis, psoriasis
p40 chain of IL-12 and IL-23	Inhibits T_H1 and T_H17 responses	Inflammatory bowel disease, psoriasis
IL-2 receptor (CD25)	Inhibits IL-2–mediated T cell proliferation	Acute graft rejection
IFN-α	May be multiple effects on T_H1 differentiation, antibody production	Systemic lupus erythematosus
IL-4	Inhibits T_H2 differentiation, IgE production	Asthma
IL-5	Inhibits eosinophil activation	Asthma

The table lists examples of antagonists against cytokines (antibodies or soluble receptors) that are approved for clinical use or in trials. IFN, interferon; IL, interleukin; TNF, tumor necrosis factor.

ARTICLES

nature medicine

Pten deletion in RIP-Cre neurons protects against type 2 diabetes by activating the anti-inflammatory reflex

Linyuan Wang[1–3], Darren Opland[4], Sue Tsai[1], Cynthia T Luk[1,3,5], Stephanie A Schroer[1], Margaret B Allison[4], Andrew J Elia[6,7], Caren Furlonger[7], Akira Suzuki[8], Christopher J Paige[2,7,9], Tak W Mak[2,6,7,9], Daniel A Winer[1,9–11], Martin G Myers Jr[4] & Minna Woo[1–3,5,11]

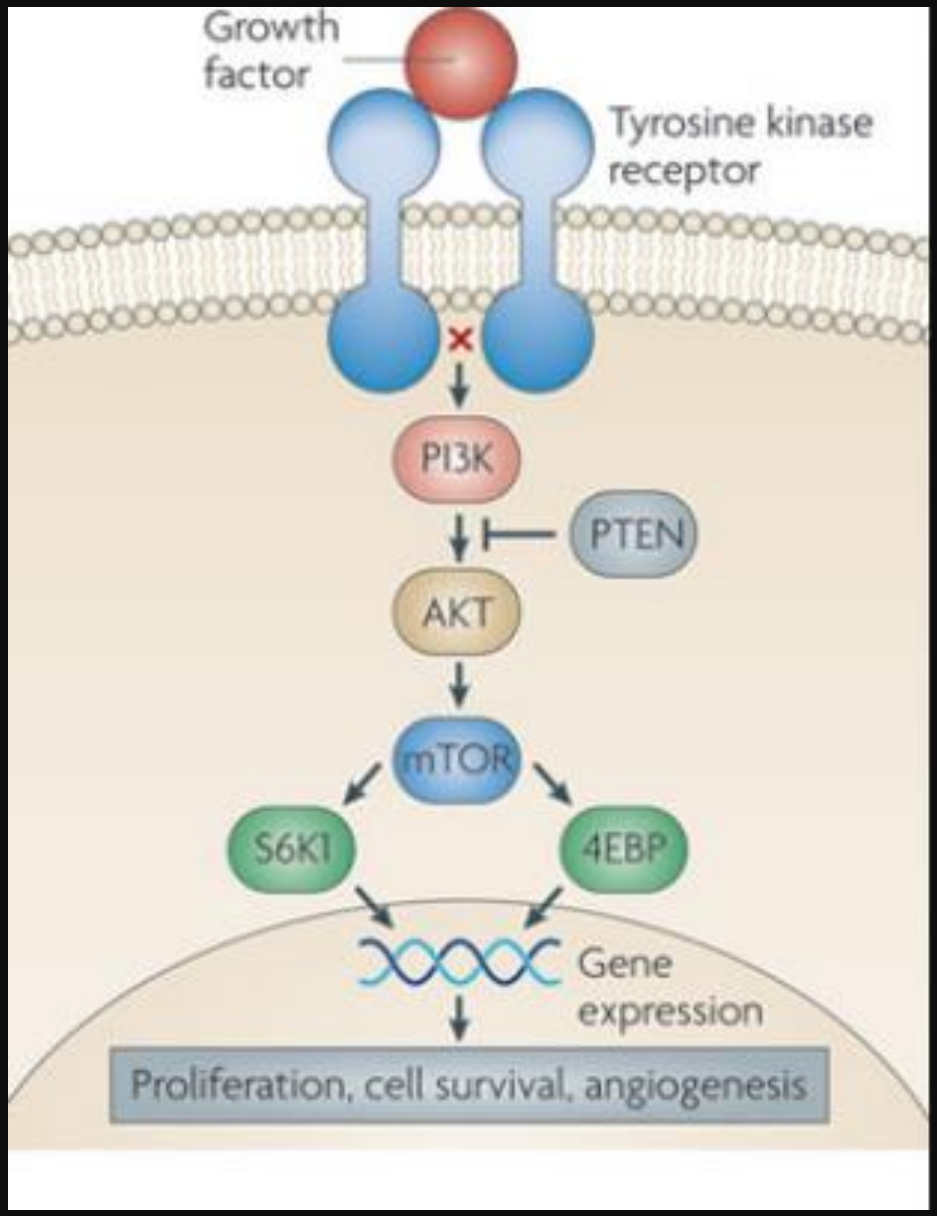

Antagônica à IP3 Kinase

Pathogenesis

- Aumento tecido adiposo
- Extravazamento de lipídeos intra celulares
- Cristais de Colesterol – TLR-4
- Ceramida – NALP3
- Hiperfosforilação de receptores
- ISR – Insulin Receptor Substrate Hiperfosforilação
- Músculo, hipotálamo, fígado

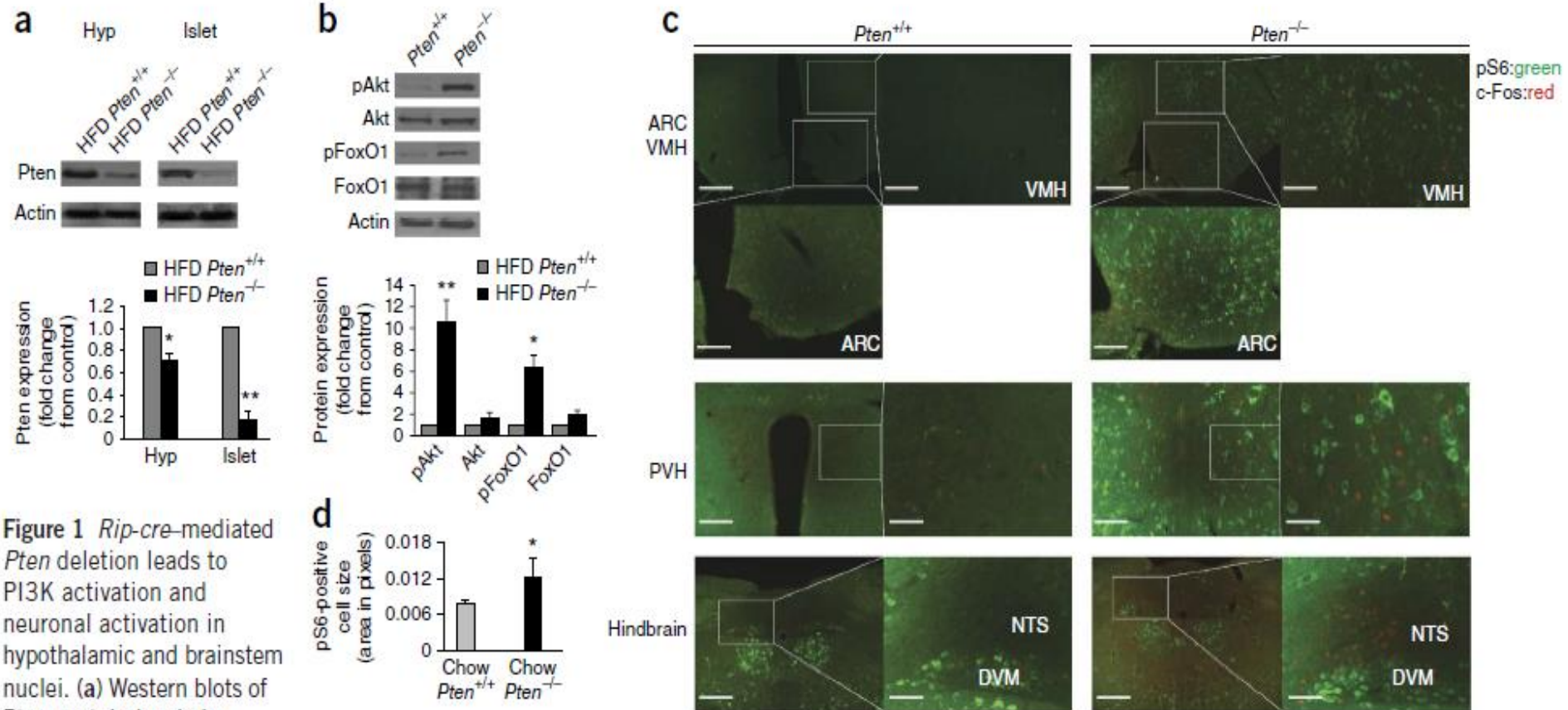

Figure 1 *Rip-cre*–mediated *Pten* deletion leads to PI3K activation and neuronal activation in hypothalamic and brainstem nuclei. (**a**) Western blots of Pten protein levels in hypothalamic (Hyp) and islet lysates (top) and quantification (bottom) in *Rip-cre*$^{+}$ *Pten*$^{+/+}$ (*Pten*$^{+/+}$) and *Rip-cre*$^{+}$ *Pten*$^{flox/flox}$ (*Pten*$^{-/-}$) mice ($n = 6$ per group). (**b**) Western blots (top) and quantification (bottom) of whole hypothalamic pAkt, total Akt, pFoxO1 and total FoxO1 from *Pten*$^{+/+}$ and *Pten*$^{-/-}$ mice ($n = 6$ per group). (**c**) Representative immunofluorescent staining of pS6 (green) and c-Fos (red) in arcuate (ARC), ventromedial (VMH) and paraventricular (PVH) nuclei of the hypothalamus (20× magnification; scale bars, 100 μm) and in NTS and DVM nuclei of the brainstem (10× magnification; scale bars, 200 μm) from *Pten*$^{+/+}$ and *Pten*$^{-/-}$ mice. (**d**) Size of pS6-postive cells in pixels from the PVH nucleus ($n = 6$ per group). All data are presented as the means ± s.e.m. $^{*}P < 0.05$, $^{**}P < 0.01$ (independent-sample *t* test).

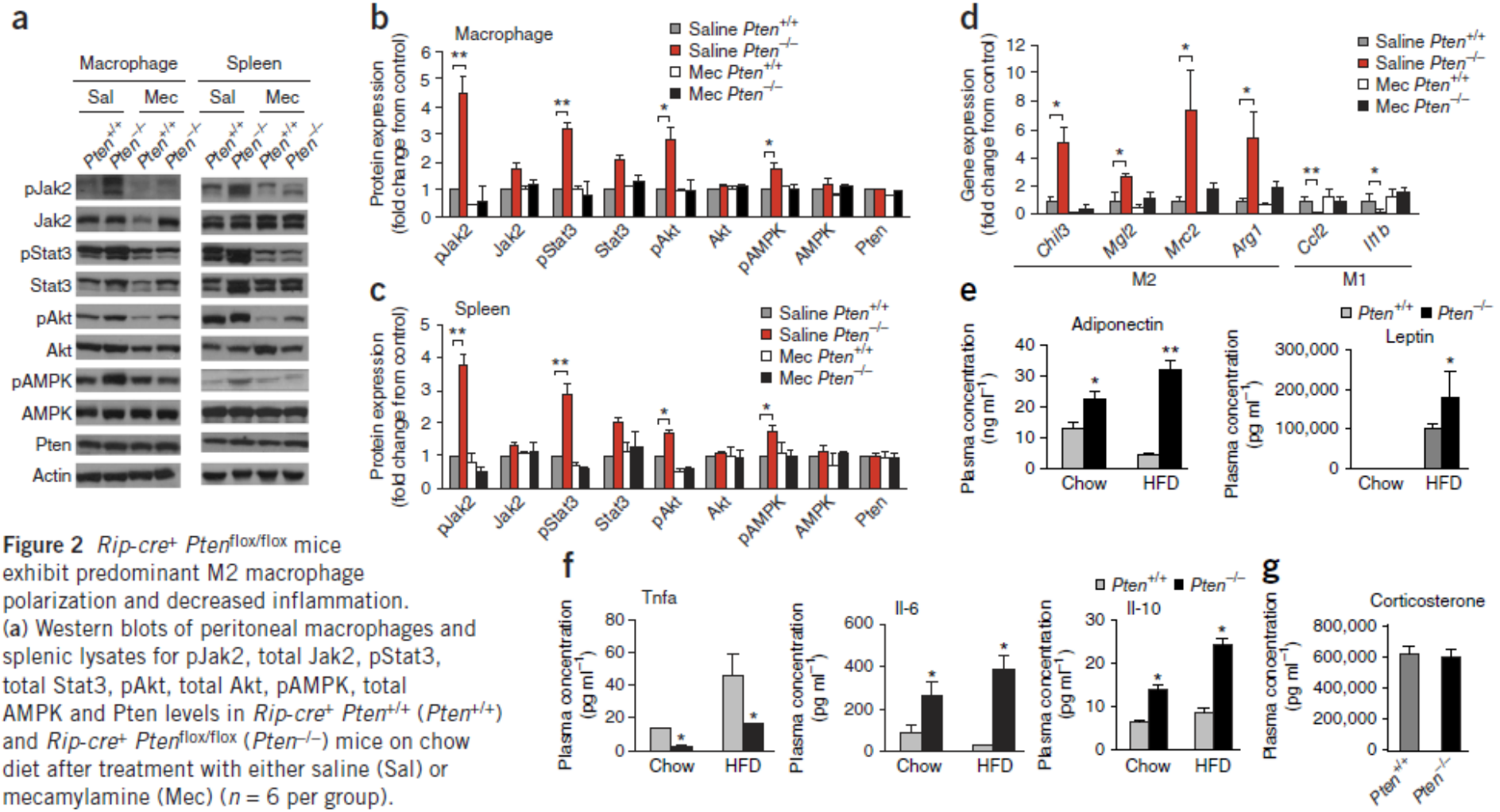

Figure 2 *Rip-cre*$^{+}$ *Pten*$^{flox/flox}$ mice exhibit predominant M2 macrophage polarization and decreased inflammation. (**a**) Western blots of peritoneal macrophages and splenic lysates for pJak2, total Jak2, pStat3, total Stat3, pAkt, total Akt, pAMPK, total AMPK and Pten levels in *Rip-cre*$^{+}$ *Pten*$^{+/+}$ (*Pten*$^{+/+}$) and *Rip-cre*$^{+}$ *Pten*$^{flox/flox}$ (*Pten*$^{-/-}$) mice on chow diet after treatment with either saline (Sal) or mecamylamine (Mec) ($n = 6$ per group). (**b**,**c**) Quantification of protein levels in peritoneal macrophages (**b**) and splenic lysates (**c**) ($n = 6$ per group). (**d**) Quantitative PCR to indicate the transcript levels of genetic markers of M2 polarized macrophages (*Chil3*, *Mgl2*, *Mrc2* and *Arg1*) and M1 macrophages (*Ccl2* and *Il1b*) in *Pten*$^{+/+}$ and *Pten*$^{-/-}$ mice on chow diet after treatment with either saline or mecamylamine ($n = 6$ per group). (**e**–**g**) Fasting plasma adipokines adiponectin (left) and leptin (right) (**e**), cytokines Tnfa (left), Il-6 (center) and Il-10 (right) (**f**) and corticosterone (**g**) in *Pten*$^{+/+}$ and *Pten*$^{-/-}$ mice on chow or HFD ($n = 10$ per group). All data are presented as the means ± s.e.m. $^{*}P < 0.05$, $^{**}P < 0.01$ (independent-sample *t* test).

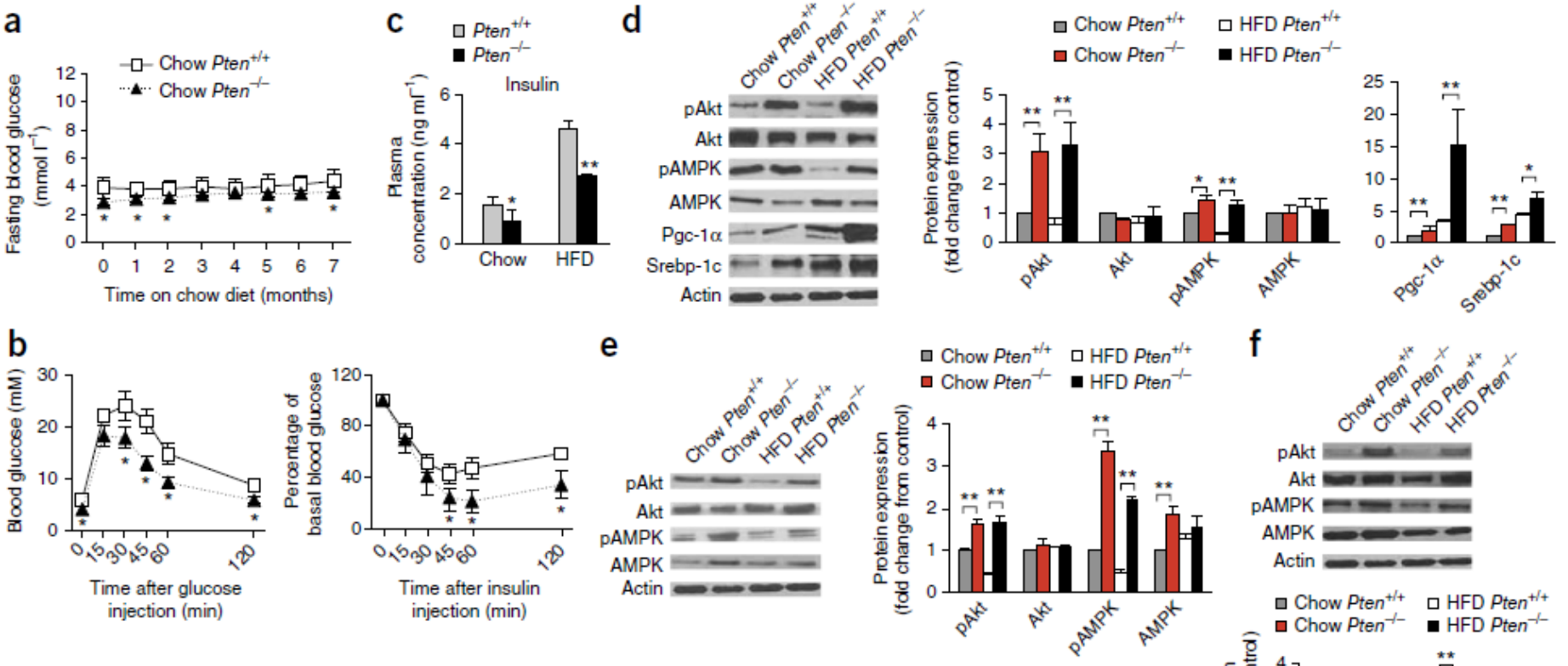

Figure 3 *Rip-cre*$^{+}$ *Pten*$^{flox/flox}$ mice have enhanced whole-body and metabolic tissue insulin sensitivity on chow and HFD. (**a**) Fasting blood glucose levels of *Rip-cre*$^{+}$ *Pten*$^{+/+}$ (*Pten*$^{+/+}$) and *Rip-cre*$^{+}$ *Pten*$^{flox/flox}$ (*Pten*$^{-/-}$) mice on 7 months of chow diet starting at 2 months of age ($n = 15$ per group). (**b**) GTT (left) of *Pten*$^{+/+}$ and *Pten*$^{-/-}$ mice after 7 months of chow diet ($n = 15$ per group) and ITT (right) of *Pten*$^{+/+}$ and *Pten*$^{-/-}$ mice after 7 months of chow diet ($n = 15$ per group). (**c**) Fasting plasma insulin concentrations from *Pten*$^{+/+}$ and *Pten*$^{-/-}$ mice on chow or HFD ($n = 10$ per group). (**d**) Western blots (left) and quantification (right) of visceral adipose tissue pAkt, total Akt, pAMPK, total AMPK, peroxisome proliferative activated receptor, γ, coactivator 1α (Pgc-1α, also called Ppargc1a) and sterol regulatory element binding transcription factor 1 (Srebp-1c, also called Srebf1) of *Pten*$^{+/+}$ and *Pten*$^{-/-}$ mice on chow or HFD ($n = 6$ per group). (**e**,**f**) Western blots (left) and quantification (right) of pAkt, total Akt, pAMPK and total AMPK in liver (**e**) and muscle (**f**; top and bottom, respectively) of *Pten*$^{+/+}$ and *Pten*$^{-/-}$ mice on chow or HFD ($n = 6$ per group). All data are presented as the means ± s.e.m. $^{*}P < 0.05$, $^{**}P < 0.01$ (independent-sample *t* test).

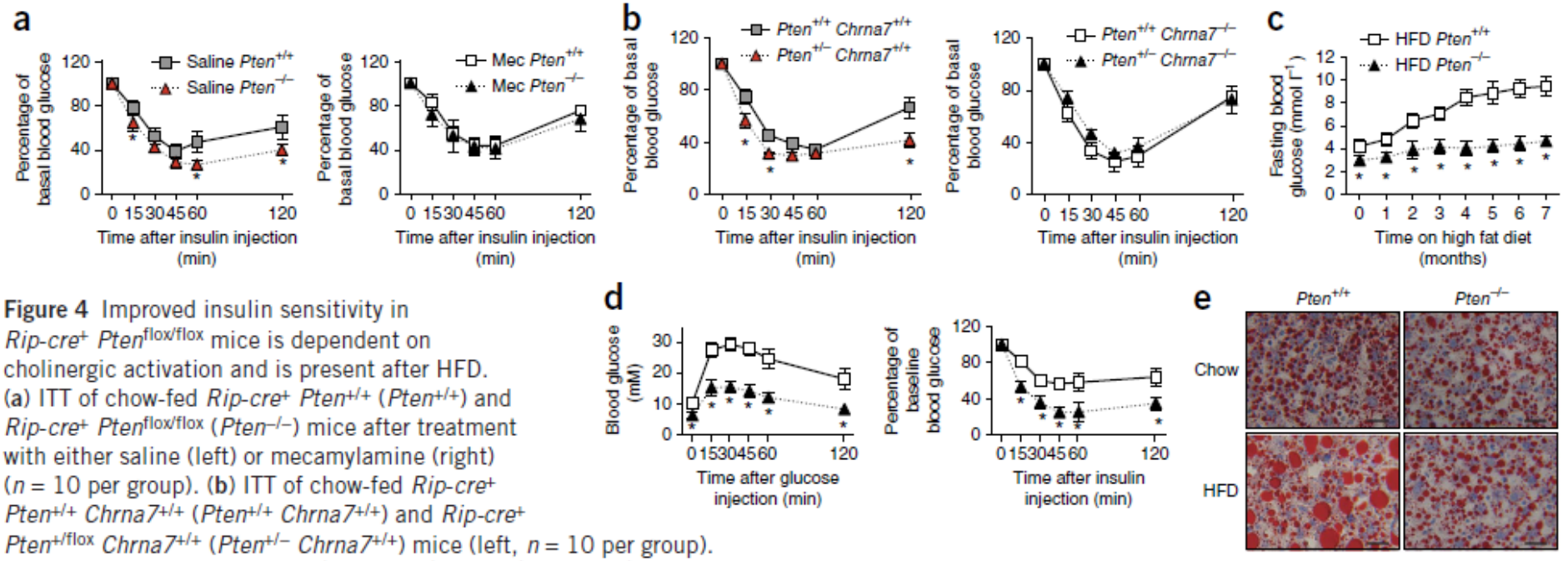

Figure 4 Improved insulin sensitivity in *Rip-cre*$^{+}$ *Pten*$^{flox/flox}$ mice is dependent on cholinergic activation and is present after HFD. (**a**) ITT of chow-fed *Rip-cre*$^{+}$ *Pten*$^{+/+}$ (*Pten*$^{+/+}$) and *Rip-cre*$^{+}$ *Pten*$^{flox/flox}$ (*Pten*$^{-/-}$) mice after treatment with either saline (left) or mecamylamine (right) ($n = 10$ per group). (**b**) ITT of chow-fed *Rip-cre*$^{+}$ *Pten*$^{+/+}$ *Chrna7*$^{+/+}$ (*Pten*$^{+/+}$ *Chrna7*$^{+/+}$) and *Rip-cre*$^{+}$ *Pten*$^{+/flox}$ *Chrna7*$^{+/+}$ (*Pten*$^{+/-}$ *Chrna7*$^{+/+}$) mice (left, $n = 10$ per group). ITT of chow-fed *Rip-cre*$^{+}$ *Pten*$^{+/+}$ *Chrna7*$^{-/-}$ (*Pten*$^{+/+}$ *Chrna7*$^{-/-}$) and *Rip-cre*$^{+}$ *Pten*$^{+/flox}$ *Chrna7*$^{-/-}$ (*Pten*$^{+/-}$ *Chrna7*$^{-/-}$) mice (right, $n = 7$ per group). (**c**) Fasting blood glucose levels of *Pten*$^{+/+}$ and *Pten*$^{-/-}$ mice on 7 months of HFD starting at 2 months of age ($n = 15$ per group). (**d**) GTT of *Pten*$^{+/+}$ and *Pten*$^{-/-}$ mice after 7 months of HFD (left, $n = 15$ per group) and ITT of *Pten*$^{+/+}$ and *Pten*$^{-/-}$ mice after 7 months of HFD (right, $n = 15$ per group). (**e**) Representative Oil Red O–stained liver sections of *Pten*$^{+/+}$ and *Pten*$^{-/-}$ mice on either chow or HFD (scale bars, 80 μm). All data are presented as the means ± s.e.m. $^{*}P < 0.05$, $^{**}P < 0.01$ (independent-sample *t* test).

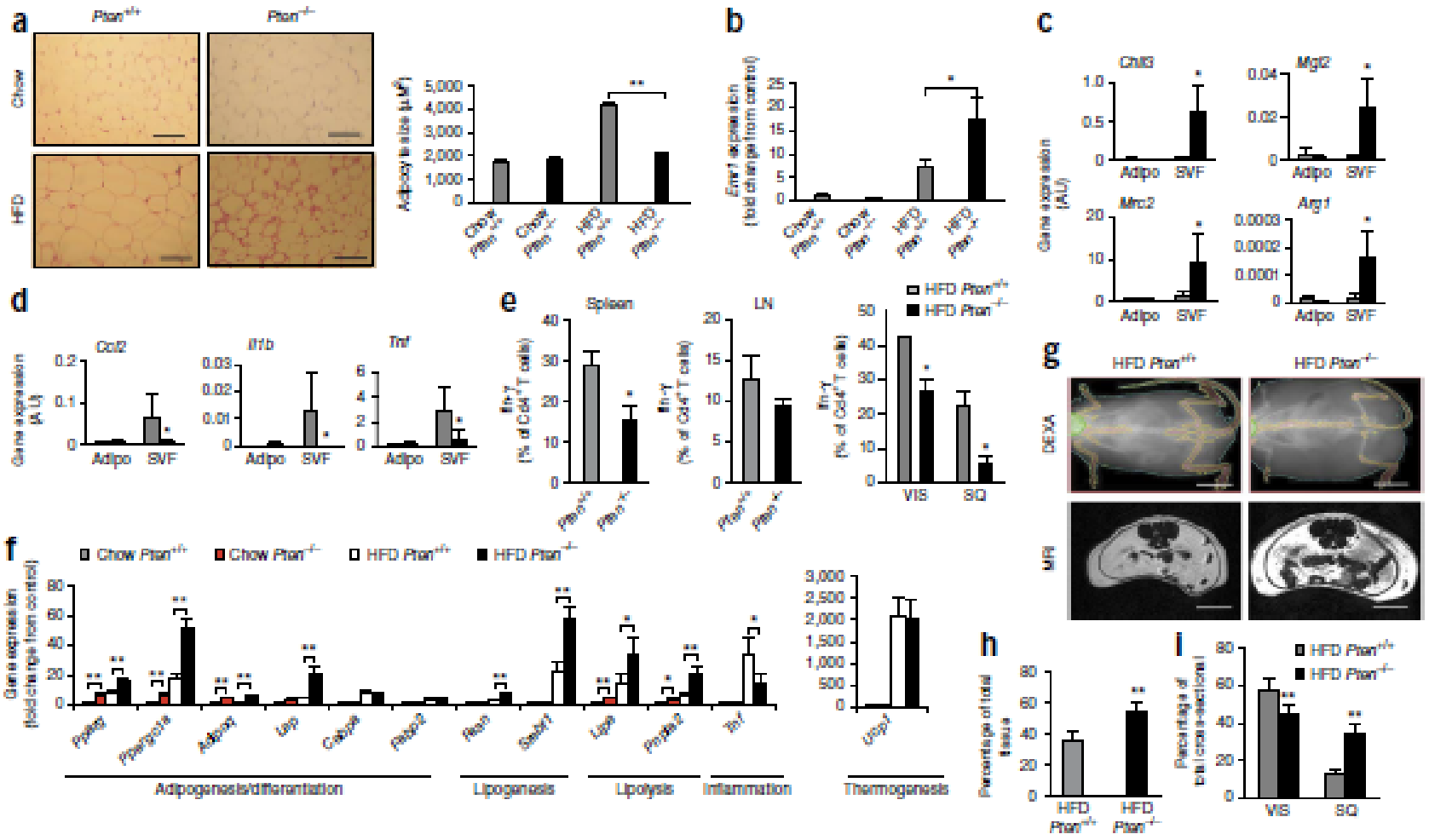

Figure 5 HFD-fed *Rip-cre*$^{+}$ *Pten*$^{flox/flox}$ mice demonstrate greater M2 macrophage infiltration and adipogenesis in the visceral compartment. (**a**) Representative H&E-stained visceral adipose tissue sections (left; scale bars, 200 μm) and quantification of adipocyte size (right) in *Rip-cre*$^{+}$ *Pten*$^{+/+}$ (*Pten*$^{+/+}$) and *Rip-cre*$^{+}$ *Pten*$^{flox/flox}$ (*Pten*$^{-/-}$) mice on chow or HFD ($n = 6$ per group). (**b**) Quantitative PCR of *Emr1* transcript levels in visceral adipocytes of *Pten*$^{+/+}$ and *Pten*$^{-/-}$ mice on chow or HFD ($n = 6$ per group). (**c**) Quantitative PCR of *Chil3*, *Mgl2*, *Mrc2* and *Arg1* transcript levels of adipocytes (Adipo) and the SVF from HFD-fed *Pten*$^{+/+}$ and *Pten*$^{-/-}$ mice ($n = 6$ per group). AU, arbitrary units. (**d**) Quantitative PCR of *Ccl2*, *Il1b* and *Tnf* transcript levels of adipocytes and the SVF from HFD-fed *Pten*$^{+/+}$ and *Pten*$^{-/-}$ mice ($n = 6$ per group). (**e**) Phorbol myristate acetate (PMA)-stimulated Ifn-γ production by CD4^{+} T cells isolated from the spleen (left), lymph node (LN) (center) and visceral (VIS) and subcutaneous (SQ) adipose tissue (right) of two to three pooled *Pten*$^{+/+}$ and *Pten*$^{-/-}$ mice on HFD ($n = 4$ per group). (**f**) Gene expression of markers for adipogenesis (*Pparg*, *Ppargc1a*, *Adipoq*, *Lep*, *Cebpa* and *Fabp4*), lipogenesis (*Fasn* and *Srebf1*), lipolysis (*Lipe* and *Pnpla2*), inflammation (*Tnf*) and thermogenesis (*Ucp1*) ($n = 6$ per group). (**g**) Representative magnetic resonance imaging (MRI) and dual-energy X-ray absorptiometry (DEXA) images of *Pten*$^{+/+}$ and *Pten*$^{-/-}$ mice after 7 months on HFD starting at 2 months of age (scale bars, 75 mm). (**h**) Percentage body fat of *Pten*$^{+/+}$ and *Pten*$^{-/-}$ mice after 7 months of HFD by DEXA ($n = 5$). (**i**) Quantification of VIS and SQ adipose tissue in cross-sectional areas of MRIs of *Pten*$^{+/+}$ and *Pten*$^{-/-}$ mice ($n = 5$). All data are presented as the means ± s.e.m. $^{*}P < 0.05$, $^{**}P < 0.01$ (independent-sample *t* test).

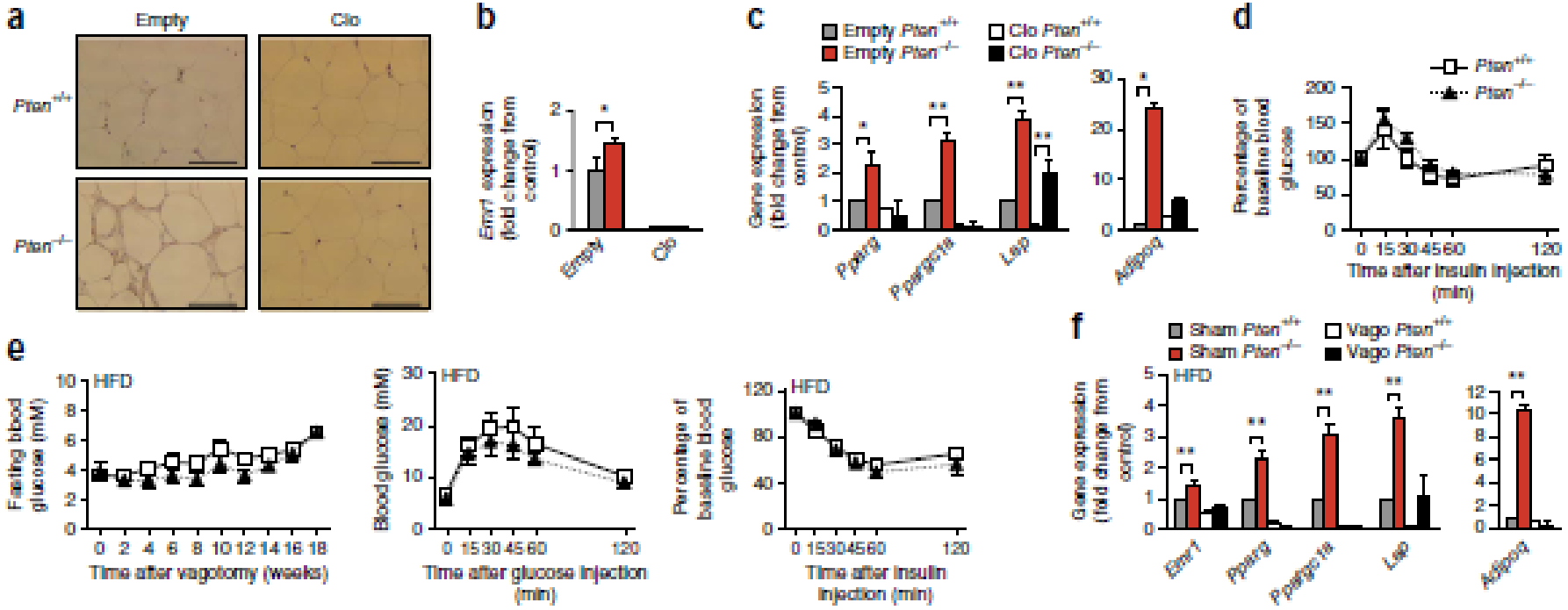

Figure 6 Macrophage depletion or vagotomy attenuates visceral adipogenesis and peripheral insulin sensitivity. (**a**) Representative immunohistochemical staining of F4/80 in visceral adipose tissue from chow-fed *Rip-cre*$^{+}$ *Pten*$^{+/+}$ (*Pten*$^{+/+}$) and *Rip-cre*$^{+}$ *Pten*$^{loxP/loxP}$ (*Pten*$^{-/-}$) mice after injection of either empty liposome (Empty) or liposome-encapsulated clodronate (Clo) (scale bars, 200 μm). (**b**) Quantitative PCR of *Emr1* (F4/80) transcript levels in visceral adipose tissue of chow-fed *Pten*$^{+/+}$ and *Pten*$^{-/-}$ mice after injection of either empty liposome or clodronate ($n = 6$ per group). (**c**) ITT of chow-fed *Pten*$^{+/+}$ and *Pten*$^{-/-}$ mice after clodronate injection ($n = 10$ per group). (**d**) Quantitative PCR of adipogenic marker (*Pparg*, *Ppargc1a*, *Lep* and *Adipoq*) gene expression levels in visceral adipose tissue of chow-fed *Pten*$^{+/+}$ and *Pten*$^{-/-}$ mice after injection of either empty liposome or clodronate ($n = 3$ per group). (**e**) Fasting blood glucose levels (left), GTT (center) and ITT (right) of vagotomized *Pten*$^{+/+}$ and *Pten*$^{-/-}$ mice after 5 months of HFD ($n = 7$). (**f**) Quantitative PCR of *Emr1*, *Pparg*, *Ppargc1a*, *Lep* and *Adipoq* gene expression levels in visceral adipose tissue of vagotomized (Vago) *Pten*$^{+/+}$ and *Pten*$^{-/-}$ mice on HFD ($n = 6$ per group). (**g**) Quantitative PCR of *Mgl2*, *Mrc2*, *Ccl2* and *Il1b* gene expression levels in visceral adipose tissue of vagotomized *Pten*$^{+/+}$ and *Pten*$^{-/-}$ mice on HFD normalized to *Emr1* levels ($n = 6$ per group). (**h**) Schematic representation of the mechanism of PI3K activation in RIP-Cre neurons mediating protection against type 2 diabetes (T2DM). All data are presented as the means ± s.e.m. $^{*}P < 0.05$, $^{**}P < 0.01$ (independent-sample *t* test).